Technical University of Denmark

Alejandro Gonzalez Pacheco

Measurements of different acoustic conditions in small rectangular rooms

Master's thesis, June 2014

DTU Electrical Engineering
Department of Electrical Engineering

Measurements of different acoustic conditions in small rectangular rooms

This report was prepared by:
Alejandro Gonzalez Pacheco

Supervisors:
Cheol-Ho Jeong, Associate Professor at Acoustical Technology, DTU Elektro
Jonas Brunskog, Associate Professor at Acoustical Technology, DTU Elektro
Gerd Høy Marbjerg, Industrial PhD student at Acoustical Technology, DTU Elektro

DTU Elektro
Electrical Engineering
Danmarks Tekniske Universitet
Ørsteds Plads
Bygning 352
2800 Kgs. Lyngby
Denmark

www: elektro.dtu.dk
Tel: (+45) 45 25 35 00
Fax: (+45) 45 88 61 11

Date of publication: June 20th, 2014

Class: 1 (public)

Edition: 1. edition

Remarks: This report was prepared in collaboration with Ecophon and it is submitted in compliance with the requirements to achieve the degree of Master of Science in Acoustical Engineering at the Department of Electrical Engineering, at the Technical University of Denmark. The report represents 30 ECTS.

PROYECTO FIN DE CARRERA

TEMA: Acústica arquitectónica. Architectural Acoustics.

TÍTULO: Medidas de diferentes condiciones acústicas en pequeñas salas rectangulares. Measurements of different acoustic conditions in small rectangular rooms

AUTOR: Alejandro González Pacheco

TUTOR: Cheol-Ho Jeong

DEPARTAMENTO: Ingeniería Acústica. Acoustics Engineering

CENTRO DE LECTURA: Danmarks Tekniske Universitet (DTU)

Fecha de Lectura: 24-07-2014

Calificación: 7

RESUMEN DEL PROYECTO:

Mediciones de Respuesta al Impulso son llevadas a cabo en las instalaciones con que cuenta la empresa Ecophon en su sede central de Hyllinge, Suecia. En una de sus salas, se recrean diferentes configuraciones típicas de aula, variando la altura y composición de los techos, colocando paneles absorbentes de pared e incluyendo diferentes elementos mobiliario como pupitres y sillas. Tres diferentes materiales absorbentes porosos de 15, 20 y 50 mm de espesor, son utilizados como techos suspendidos así como uno de 40 mm es utilizado en forma de paneles. Todas las medidas son realizadas de acuerdo al estándar ISO 3382, utilizando 12 combinaciones de fuente sonora y micrófono para cada configuración, así como respetando las distancias entre ellos establecidas en la norma. El objetivo de toda esta serie de medidas es crear una base de datos de parámetros acústicos tales como tiempo de reverberación, índice de claridad o índice de inteligibilidad medidos bajo diferentes configuraciones con el objeto de que éstos sirvan de referencia para la validación de una nueva herramienta de simulación acústica llamada PARISM que está siendo desarrollada en este momento en la Danmarks Tekniske Universitet de Copenhague. Esta herramienta tendrá en cuenta la fase, tanto en propagación como en reflexión, así como el comportamiento angulodependiente de los materiales y la difusión producida por las superficies.

Las diferentes configuraciones de aula recreadas en Hyllinge, son simuladas también utilizando el software de simulación acústica ODEON con el fin de establecer comparaciones entre medidas y simulaciones para discutir la validez de estas ultimas. La información resultante es esencial para el desarrollo de la nueva herramienta de simulación, especialmente los resultados por debajo de la frecuencia de corte de Schroeder, donde ODEON no produce predicciones precisas debido a que no tiene en cuenta la fase ni en propagación ni en reflexión.

La impedancia de superficie de los materiales utilizados en los experimentos, todos ellos fabricados por la propia empresa Ecophon, es medida utilizando un tubo de Kundt. De este modo, los coeficientes de absorción de incidencia aleatoria son calculados e incorporados a las simulaciones. Además, estos coeficientes también son estimados mediante el modelo empírico de Miki, con el fin de ser comparados con los obtenidos mediante otros métodos. Un breve estudio comparativo entre coeficientes de absorción obtenidos por diversos métodos y el efecto producido por los materiales absorbentes sobre los tiempos de reverberación es realizado. Grandes diferencias son encontradas, especialmente entre los métodos de tubo de impedancia y cámara reverberante. La elección de reacción local o extendida a la hora de estimar los coeficientes también produce grandes diferencias entre los resultados.

Pese a que la opción de absorción angular es activada en todas las simulaciones realizadas con ODEON para todos los materiales, los resultados son mucho más imprecisos de lo esperado a la hora de compararlos con los valores extraidos de las medidas de Respuesta al Impulso. En salas como las recreadas, donde una superficie es mucho más absorbente que las demás, las ondas sonoras tienden a incidir en la superficie altamente absorbente desde ángulos de incidencia muy pequeños. En este rango de ángulos de incidencia, las absorciones que presentan los materiales absorbentes porosos estudiados son muy pequeñas, pese a que sus valores de coeficientes de absorción de incidencia aleatoria son altos. Dado que como descriptor de las superficies en ODEON se utiliza el coeficiente de absorción de incidencia aleatoria, los tiempos de reverberación son siempre subestimados en las simulaciones, incluso con la opción de absorción angular activada. Esto es debido a que el algoritmo que ejecuta esta opción, solo tiene en cuenta el tamaño y posición de las superficies, mientras que el comportamiento angulodependiente es diferente para cada material. Es importante destacar, que cuando la opción es activada, los tiempos simulados se asemejan

más a los medidos, por lo tanto esta característica sí produce ciertas mejoras pese a no modelar la angulodependencia perfectamente.

Por otra parte, ODEON tampoco tiene en cuenta el fenómeno de difracción, ni acepta longitudes de superficie menores de una longitud de onda a frecuencias medias (30 cm) por lo que en las configuraciones que incluyen absorbentes de pared, los cuales presentan un grosor de 4 cm que no puede ser modelado, los tiempos de reverberación son siempre sobreestimados. Para evitar esta sobreestimación, diferentes métodos de correción son analizados.

Todas estas deficiencias encontradas en el software ODEON, resaltan la necesidad de desarrollar cuanto antes la herramienta de simulación acústica PARISM, la cual será capaz de predecir el comportamiento del campo sonoro de manera precisa en este tipo de salas, sin incrementar excesivamente el tiempo de cálculo.

En cuanto a los parámetros extraidos de las mediciones de Respuesta al Impulso, bajo ninguna de las configuraciones recreadas los tiempos de reverberación cumplen con las condiciones establecidas por la regulación danesa en materia de edificación. Es importante destacar que los experimentos son llevados a cabo en un edificio construido para uso industrial, en el que, pese a contar con un buen aislamiento acústico, los niveles de ruido pueden ser superiores a los existentes dentro de el edificio donde finalmente se ubique el aula. Además, aunque algunos elementos de mobiliario como pupitres y sillas son incluidos, en una configuración real de aula normalmente aparecerían algunos otros como taquillas, que no solo presentarían una mayor absorción, sino que también dispersarían las ondas incidentes produciendo un mejor funcionamiento del techo absorbente. Esto es debido a que las ondas incidirían en el techo desde una mayor variedad de ángulos, y no solo desde ángulos cercanos a la dirección paralela al techo, para los cuales los materiales presentan absorciones muy bajas o casi nulas.

En relación a los otros parámetros como índice de claridad o índice de inteligibilidad extraidos de las medidas, no se han podido extraer conclusiones válidas dada la falta de regulación existente. Sin embargo, el efecto que produce sobre ellos la inclusión de techos, paneles de pared y mobiliario sí es analizada, concluyendo que, como era de esperar, los mejores resultados son obtenidos cuando todos los elementos están presentes en la sala en el mismo momento.

Abstract

Impulse response measurements are carried out in laboratory facilities at Ecophon, Sweden, simulating a typical classroom with varying suspended ceilings and furniture arrangements. The aim of these measurements is to build a reliable database of acoustical parameters in order to have enough data to validate the new acoustical simulation tool which is under development at Danmarks Tekniske Universitet, Denmark. The different classroom configurations are also simulated using ODEON Room Acoustics software and are compared with the measurements. The resulting information is essential for the development of the acoustical simulation tool because it will enable the elimination of prediction errors, especially those below the Schroeder frequency.

The surface impedance of the materials used during the experiments is measured in a Kundt's tube at DTU, in order to characterize them as accurately as possible at the time of incorporation into the model.

A brief study about porous materials frequently used in classrooms is presented. Wide differences are found between methods of measuring absorption coefficients and local or extended assumptions.

First, I would like to express my gratitude to each and every one of my supervisors for the help and depth of understanding that they have given me throughout the year. In addition to Cheol-Ho Jeong, Jonas Brunskog, and Gerd Høy Marbjerg, I would like to thank Erling Nilsson and the Ecophon company for the incredible opportunity that they have provided me with by allowing me to work on this project, during which I have learned practically all of what I currently know about Architectural Acoustics. I would also like to thank Tom Arent Peterson and Jørgen Rasmussen for the technical support that they have given me, and, not only for being available, but for responding to all of my inquiries with a smile and friendly disposition. In addition, a thank you to Efrén Fernández, who has guided my thinking and my personal growth, even before I arrived in Denmark. I am also grateful to my colleagues, Kristrún and Mélanie, who have helped me to complete this work by sharing their extensive knowledge with me. I would be remiss if I neglected to thank my family for the sacrifices that each of them have made so that I could study here in Copenhagen during this year. They are a constant source of support and inspiration for me to continue with my studies. Lastly, I would like to encourage Gerd to continue with her work as she has done so far. I am certain that her work-ethic will take her far, not only with this project, but with any other and all future work.

Contents

CHAPTER 1

Introduction

1.1 Motivation and goals

A new room acoustics simulation tool is under development at DTU, which is able to model the acoustics in small rectangular rooms. The project is being carried out in collaboration with the company Ecophon, a producer of porous absorbers for ceilings and walls. This tool will be used to predict the non-diffuse sound fields created in rooms with highly absorbent ceilings, such as classrooms or offices. It is well known that in this kind of room, the Sabine equation does not predict the sound field accurately since the absorbing surfaces show an angle-dependent behaviour. Furthermore, most of the models that are currently being used do not take into account the phase in propagation and reflection. The new model, called PARISM [1], will overcome these shortcomings including impedance as a descriptor of the surfaces, phase in reflection and propagation and both specular and diffuse reflections.

In order to validate the model, measurements of some acoustical properties in rooms need to be compared with the predictions. This is the purpose of this Master Thesis, the main objective of which is to build a reliable database of measurements of these acoustical parameters under different conditions. The configurations will also be simulated using Odeon Room Acoustics software with the objective of highlighting the need to developing the new PARISM.

1.2 State of the Art

The works of Spändok and Meyer [2, 3], who carried out the first acoustical simulations in the 1930s, can be considered the basis of what today are known as acoustical simulation tools. It was not until the 1960s that the first computational calculations were performed. In 1962 [4], the Ray Tracing Method was presented. This is a geometrical method that shows the energy propagation in an enclosed space. It models diffuse reflections following Lambert's Law, whereby each time a ray hits a surface, its energy is reflected in multiple directions and is attenuated by the absorption coefficient of the surface. It was later, in 1985 [5], when this method was adopted by the acousticians. In the same year, different variations appeared, such as the Beam Tracing model [6]. In the 1970s, the first Intelligibility Index calculations were performed, as well as reverberation time predictions in a simple rectangular room [7]. In the same decade, the Radiosity method [8] was integrated into acoustics. This method, which was presented in the 1920s as a useful tool in the lighting field, has been applied from 1993 to today to run acoustical simulations [9]. It is one of the methods in use nowadays that has as a major drawback its high computational time. The latest important method used these days, Image Source [10], was proposed in 1979. Based on the statistical theory, this works by creating a set of sources which are symmetrical to the original one. Each of these image sources acts as a new one when a ray hits a reflective surface, which is the axis of symmetry between the real and the image source. The main disadvantages are its limitation to regular shaped rooms, and high increment in computational time when the reflection order is increased.

In 1984, the ODEON project began, as a collaboration between Danmark Tekniske Universitet and a group of consulting companies in order to move forward on acoustical simulations and develop a commercial software. Some years later, in 1989, this laboratory developed the first hybrid model combining Image Source and Ray Tracing methods [11]. For a ray path, its reflection on each surface is calculated making use of the Image Source method adding, at the same time, the effect of diffusion modelled using the Ray Tracing algorithm. Thus, better results are obtained with a lower computational time. The new hybrid model was implemented as a software (ODEON 1.0). This was the first version of the Room Acoustic ODEON software. Based on this model, other developers launched at a later stage different products (RAYSCAT / EASE).

At that moment a yet unfinished race towards the optimization of the models started. In the early 1990s, auralization, one of the most innovative concepts in acoustics emerged[12]. As a product of convolution between a simulated impulse response and a sound signal previously recorded in an anechoic chamber, this method allows the user to listen to how this signal would sound in an exact point of a known room or even in a non-existent room. ODEON included this feature in its next software version. Many different improvements to the hybrid model, such as adding statistical calculations for large volumes, or applying Finite Element theory to optimize diffusion calculations [13], were successively appearing.

Since that time, several hybrid simulation tools combining different methods have been used in order to obtain accurate sound field predictions in all types of rooms. Such tools include numerical models (BEM / FEM) [14], as well as wave models [15], which are able to take phase into account. Both are only valid at low frequencies, since the computational time is excessively high. Other simulation tools, such as SEA [16], or mathematical solutions, like transfer matrix [17], have been adapted to acoustics and shown to be very convenient for certain applications.

Thus, a wide variety of acoustical simulation tools are available nowadays, each presenting a number of advantages and drawbacks, especially under different configurations of rooms and materials. Knowing the disadvantages of these tools when simulating non diffuse sound fields as found in classrooms and offices, the new PARISM model, goes a step further to improve the accuracy of the simulations without increasing computational time.

1.3 Structure of the Thesis

After this short introduction, Chapter 2 explains the different methods applied in measurements and calculations to obtain the acoustical parameters needed. Furthermore, it includes some theoretical concepts that can not be omitted and will help the understanding of the global concept of this Master Thesis. In Chapter 3, the most relevant results found by these processes are reported. All data are analysed and discussed in Chapter 4, followed by a summary in Chapter 5.

The complete results of measurements, calculations and simulations are presented in Appendices.

CHAPTER 2

Theories and methods

2.1 Classroom acoustics

Although the negative effect on students by poor acoustic conditions in classrooms has been investigated for many years and has been indisputably demonstrated [18], most schools do not spend the money and time required to improve the situation. This is due to lack of information about this topic, and the difficulty of relating bad academic results to the acoustics. To give an example, if a blackboard is so old that the numbers written on it can not be recognised by the students, the teacher will realize this and the blackboard will be changed. However, in many cases, teachers who have always been teaching in the same classrooms with bad acoustic conditions do not think that the students may not be receiving their message correctly because of a low speech intelligibility level in the room.
Solving this kind of situations is sometimes expensive, as in the case of a ceiling change, but very often, solutions are as simple as placing some absorbers in the room to avoid disturbing sound reflections or installing a small reflective surface in order to reinforce the direct sound. In addition to the lack of information on this issue, the widespread belief that considers external and equipment noises as the only noise sources to be taken into consideration when designing a classroom, has meant that most of the acoustic improvements made in these rooms have been focused on building isolation. On certain occasions, these changes have not produced any improvement, since one of the noise sources that may result in worse acoustic conditions and which therefore deserves to be treated carefully, is the noise caused by the students themselves [19]. This does not mean that classrooms do

not have to be treated to prevent a high background noise level caused by external noise, but an effort should be made to avoid the effect of noise generated inside the room, which can be as damaging as the effect caused by any external source.

A certain number of general acoustic conditions should be guaranteed in a room in order to ensure good speech intelligibility [20, 21]:

- Adequate loudness level
- Low background noise
- Low reverberant sound field level
- Absence of acoustical defects such as echoes, focusing and flutter echoes

These conditions are the same for any speech room, although there may be some differences between them, as in the case of offices, where a high level of privacy is desirable. By fulfilling the two first requirements, a high signal-to-noise ratio is guaranteed. But the last two are not less important, since a high reverberation or the presence of acoustical defects could produce masking, resulting in a poorer intelligibility. Furthermore, it is extremely important that all of them present a uniform distribution throughout the entire room. Small level differences depending on the source-receiver distance can be allowed, but significant level differences between positions must be completely avoided.

An adequate level of loudness can be achieved easily without a great economic investment in acoustical treatment. In general, classrooms are spaces with a reduced volume, where the source-receiver distance does not cause excessive loudness changes. Therefore, in most cases, an electroacoustic amplification is not necessary. In order to reinforce the sound level, the placing of reflective surfaces close to the source to reflect the energy towards the receivers is highly recommended. In most cases, the presence of hard walls or even the blackboard is enough, although in certain classrooms, the installation of a small reflective surface covering part of the ceiling may be required. Its position must be carefully chosen ensuring that early reflections reach the receivers with a delay between 30 and 50 milliseconds, when they are integrated together with the direct sound by the human ear thereby reinforcing the level.

A high level of background noise must be avoided in its two components, external and internal. Generally, the necessary actions in order to avoid a high noise

level coming from outside the building, or even from other rooms of the building, are taken respecting the laws of each country, which set a series of maximum noise level values allowed for different types of rooms.

Regarding internal sources of noise, three different types can be found in a typical classroom: noise caused by electronic equipment, noise produced by ventilation systems and noise caused by the students themselves. The first two are easy to reduce by means of noise control techniques, but the third is unpredictable and much more difficult to control. Applying a treatment to reduce the level of such noise is difficult, since an extra addition of absorbent material to the room, could result in reduced sound level coming from the source, without achieving any improvement in signal-to-noise ratio.

Different reverberation times are expected depending on the use for which the classroom is intended. Longer reverberation times will be desirable for music lessons, although in most schools, all the courses are taught in the same classrooms. The control of reverberation is one of the areas where the most progress has been made, since reverberation time has been traditionally considered as the only indicator of the acoustic quality of a room. For this reason, there is a wide variety of absorbent products, which can be installed as ceilings or wall absorbers in order to achieve low reverberation times in a broad frequency bandwidth.

Acoustic defects such as echoes, focusing and flutter echoes, as well as an excessive coloration of the room should be avoided. These phenomena significantly reduce speech intelligibility and are annoying to listeners. Avoiding these defects can be quite easy during the design stage, by modifying the geometrical characteristics of the room, but it becomes harder if the room is already built. A specific solution is required for each case. It is common to use absorbent materials or diffusers in certain positions, trying to avoid the specular reflections causing these disturbing effects.

2.1.1 Acoustical parameters

The impulse responses measured in the simulated classroom are processed. A number of acoustical parameters that characterize the room and allow comparisons between different configurations are extracted. Simulations and measurements are also compared. For the development of this Thesis, the parameters are obtained

according to ISO 3382-1 [22], ISO 3382-2 [23] and IEC 60268-16 [24]. Due to the lack of information regarding the requirements to be fulfilled by the impulse responses in order to obtain these parameters, Impulse Response to Noise Ratio is used as an indicator of the validity of the measurements. By maximizing the INR values, higher precision in the results is obtained, since , as has been demonstrated [25], low values of this indicator may result in small detectable changes in the parameter values (JNDs).

For many years, reverberation time has been considered as the only indicator needed to describe the acoustic quality of a room. That is why most regulations regarding maximum allowable values for different types of rooms refer only to this parameter [26] or maximum values of background noise. This custom has been changing in recent years. Nowadays, EDT is considered to be the best descriptor of perceived reverberance [27], and other parameters, such as Speech Clarity or Sound Strength [28]. This change in mentality is based on studies showing that, while different configurations of material can produce identical reverberation times, large differences in these other parameters values are found. Furthermore, the human brain processes the early part of the decay curves in a more efficient way. Therefore, the sound pressure information received in the initial moments is critical.

RT: reverberation time is defined as the time, in seconds, required for the sound pressure level in a room to decrease by 60 dB from its initial level. Its value is extracted from the decay curve, by selecting a section of the curve from -5 dB to at least 10 dB above the background noise level. As obtaining signal-to-noise ratios over 45 dB is unusual , especially at low frequencies, the time interval is generally chosen from -5 dB to -25 dB (T_{20}) or from -5 dB to -35 dB (T_{30}). These times are then extrapolated to 60 dB. The result is the value of the reverberation time. The decay curve for each frequency band is obtained by filtering the backward integration of the squared impulse response in octave bands.

Reverberation time values are frequency dependent. They are generally lower at high frequencies in a classroom, because of the more absorbent behavior of the materials within this range and also because of absorption by the air . Furthermore, in the presence of furniture and people, these times decrease, due to the absorbent and diffusive characteristics of both. Variations depending on the amount and position of absorbers in classrooms have been studied [29].

Despite the existence of other parameters related to the perception of reverberation by the listener, RT is still the most widely used quality descriptor in all types of rooms, due to its simplicity of measurement and the extensive existing knowledge about it. Besides, acoustic regulations usually refer to this parameter. In the case of the Danish building regulation for classrooms, a maximum T_{20} value of 0.6 seconds measured according to ISO 3382-2 has to be achieved within the frequency range [125-4000] Hz. A 20% of variation for the 125 Hz octave band is allowed.

EDT: the definition is similar to that of the reverberation time. The difference lies in the choice of the decay curve section. In this case, the time that sound pressure level needs to be reduced by 10 dB is multiplied by 6. In rooms having a diffuse sound field, values of Early Decay Time and RT should be identical. Classrooms with highly absorbing surfaces produce a different value. This is because of the different slopes found in the decay curves. While RT normally presents the same values in any position, EDT depends on source-receiver distance, since, in positions close to the source, the sound energy drops abruptly at first and then begins to decrease more slowly [30]. The Standard establishes a relative JND of 5% for both reverberation time and EDT.

C_{50}: this is the logarithmic ratio of the sound energy received during the first 50 milliseconds and to the rest of the energy received at the same position. It is expressed in dB and defined by:

$$C_{50} = 10\ log \frac{\int_0^{50ms} h(t)^2\, dt}{\int_{50ms}^{\infty} h(t)^2\, dt} \quad [dB]$$

This parameter quantifies the effect of early reflections, which are the most important for determining clarity of speech . As for RT and EDT, C_{50} values are closely related to the amount and position of absorbing materials [31].

C_{50} is also related to another parameter, called Definition, which calculates the ratio between the sound energy received in the first 50 milliseconds and the total sound energy received. Both parameters are related as follows:

$$C_{50} = 10\ log \frac{D_{50}}{1 - D_{50}} \quad [dB]$$

While the Standard sets a JND value of 0.05 for D_{50}, a value for C_{50} is not specified. Therefore, the JND value of 1 dB established for C_{80} is chosen as a reference.

G: is defined as the logarithmic ratio of the impulse response sound energy to that of the response measured in a free field at a distance of 10 meters from the sound source, and given by:

$$G = 10\ log \frac{\int_0^\infty h(t)^2\, dt}{\int_0^\infty h_{10m}(t)^2\, dt} \quad [dB]$$

The sound source needs to be calibrated carefully before obtaining this parameter which is related to the contribution of the room to the perceived loudness. A JND of 1 dB is specified.

STI: this is a physical quantity representing the transmission quality of speech in relation to intelligibility. It is based on the determination of the modulation transfer function for 98 data points, obtained for 14 modulation frequencies. Following a complex process that takes into account signal-to-noise ratio values for each band of frequencies, the result is expressed as a single value. Its simplified version, the Room Acoustics Speech Transmission Index, reduces the amount of modulation frequencies as well as the number of frequency bands. This also gives a single value as result. The Standard recommends the use of a directional source simulating the directivity of the human voice, as well as the application of filters to shape the excitation signal. Since none of these recommendations have been followed during the experiments referred to in this Thesis, values of Speech Transmission Index and RASTI may be erroneous. Rating of intelligibility based on STI values can be found in Table 2.1.

Bad	**Poor**	**Fair**	**Good**	**Excellent**
0 - 0.3	0.3 - 0.45	0.45 - 0.6	0.6 - 0.75	0.75 - 1

TABLE 2.1: Intelligibility based on STI values

2.2 Porous absorbers

Despite the large variety of existing absorptive materials, this project focuses only on porous absorbers, as these are most commonly found in the acoustical treatment of classrooms. In these rooms, the diffusion is produced by furniture, so, the only non-absorptive element sometimes introduced is a small reflective surface which is beyond the scope of this work.

All the porous absorbers used to carry out the experiments described in this Thesis, are produced by the company Ecophon, a manufacturer of sound absorbing materials for ceilings and walls. This company, with headquarters in Hyllinge, Sweden, is considered worldwide as one of the leading producers of this kind of material. These materials are mainly made of glass wool, which consists essentially of glass fibers made into a texture similar to wool [32]. Its acoustic absorption is determined by multiple factors such as the dimensions and orientation of the fiber. It is an anisotropic material, generally distributed in the form of panels. The absorption varies depending on physical properties such as thickness, density, porosity and the distance to a hard surface [33]. In the typical classroom setting, absorbent materials are generally placed as a suspended ceiling. Sometimes however it is also necessary to add absorbing panels to walls, usually the rear wall. Adding too much absorption to walls, especially in positions close to the students, may cause an undesired effect on acoustic conditions, decreasing the sound pressure level excessively at those points.

Absorption variations depending on the thickness and position of the materials, are due to the fact that a rigid wall causes no particle velocity around it. As the distance d between wall and material increases, so does the particle velocity until it reaches the distance $d = \lambda/4$, where the velocity is at its maximum. A maximum in particle velocity implies maximal absorption and vice versa. This is not a problem at high frequencies, since small distances or thicknesses can comprise several particle velocity maximums. However, to achieve an effective absorption at medium and low frequencies it is necessary to increase the thickness of the material or the distance to the wall with an air cavity between them. This is the effect caused when installing suspended ceilings. It is important to keep in mind that increasing the absorption at low frequencies by separating the absorber may cause a decrease in the absorption at higher frequencies.

Regarding the density of the panel, when the values are low, few friction losses occur within the material, and thus the absorption is not effective. As density increases, a progressive increment of absorption occurs up to a limit value, at which the absorption starts to be reduced, due to the difficulty that the sound wave encounters when crossing the material.

A similar effect occurs regarding porosity, since an increase of this property permits a greater incidence of sound energy into the material and therefore a higher absorption. There is no limit value for this parameter, with values around the unity for all the absorbers.

On certain occasions, absorption coefficients larger than 1 may exist. This should not lead to the totally erroneous interpretation from a physical point of view, that the absorbed energy is greater than the incident energy. This is justified by the existence of a diffraction effect, also known as edge effect, which causes the effective area of the material to be greater than the actual area. A change is produced in the direction of the propagation of the sound wave, so that instead of being reflected, it surrounds the materials and follows its path in another direction. Small differences are produced when using in normal rooms materials whose absorption has been measured by the reverberation chamber method [34]. Discrepancies may also be found in acoustic simulations, since prediction models do not take this phenomenon into account.

2.2.1 Local and extended reaction

One of the topics that is being most investigated nowadays, is the local or extended reaction assumption when modelling a surface [35]. As a general rule, if the sound wave propagates within a material in a direction perpendicular to the surface for any angle of incidence, the material can be modelled as local. This means that the behaviour at each point is independent of behaviour at any other point. Thus, the surface impedance will also be independent of the incidence angle. Therefore, the random incidence absorption coefficients necessary for simulations are calculated easily, provided that the normal surface impedance values are known.

In contrast with the local reaction assumption, a surface can be considered as extended if the sound wave propagates within the material at an angle to the normal component which follows Snell's Law. Several studies [15] show that for

multilayer systems, such as the suspended ceilings backed by an air cavity found in many classrooms, the extended reaction assumption models the overall system performance more accurately.

The absorbing materials used during the development of the current project have been considered as homogeneous and isotropic fluids in order to characterize them using Miki's empirical model [36]. This model slightly modifies the relationships established by Delany and Bazley to extend the valid range of values, since the first equations are only valid within the range:

$$0.01 < \frac{f}{\sigma} < 1$$

When the flow resistivity values of the materials (σ) are known, the characteristic impedance, Z_c, and complex wave number in the equivalent fluid medium, k_t, are obtained by using:

$$Z_c = \rho_0 c_0 \left(1 + 0.070 \left(\frac{f}{\sigma}\right)^{-0.632} - j0.107 \left(\frac{f}{\sigma}\right)^{-0.632}\right)$$

$$k_t = \frac{w}{c_0} \left(1 + 0.109 \left(\frac{f}{\sigma}\right)^{-0.618} - j0.160 \left(\frac{f}{\sigma}\right)^{-0.618}\right)$$

being ρ_0 the density of the air, c_0 the speed of sound and j the imaginary unit.

The surface impedance of the whole system (absorber of thickness d backed by an air cavity of depth d_0) is then calculated by:

$$Z(f, \theta_i) = \frac{Z_c k_0}{k_x} \left[\frac{-jZ_{x=d} cot(k_x d) + Z_c k_0/k_x}{Z_{x=d} - jZ_c(k_0/k_x) cot(k_x d)}\right]$$

where k_0 is the wave number in air, and $k_x = \sqrt{k_t^2 - k_0^2 sin^2\theta_i}$ (normal component of k_t).

The effect of the air cavity has to be taken into account by using:

$$Z_{x=d} = -j(\rho_0 c_0 k_0/k_x) cot(k_0 d_0 cos\theta_i)$$

The next step would be to estimate the angularly varying absorption coefficients from surface impedance values, by the equation:

$$\alpha(f, \beta_i) = 1 - \left| \frac{Z(f, \theta_i) - \rho_0 c_0 / cos\beta_i}{Z(f, \theta_i) + \rho_0 c_0 / cos\beta_i} \right|^2$$

Finally, Paris' Formula is used, thereby obtaining the values of random incidence absorption coefficients in order to characterize the absorption properties of surfaces in ODEON:

$$\alpha_{random}(f) = \int_0^{\frac{\pi}{2}} \alpha(f, \beta) sin(2\beta) d\beta$$

When assuming local reaction, θ_i must be replaced by 0, since the surface impedance of the material is the same for all angles of incidence and equal to the normal incidence value. It is important to note that, despite this, the absorption coefficients vary depending on the incidence angle (β).

At this point, random incidence absorption coefficients for each octave frequency band can be estimated by two different methods. The first one involves averaging the absorption coefficients over each octave band. The second method obtains a single value of surface impedance by averaging the values of surface impedance over each octave band so as to obtain the absorption coefficient from that value. This procedure reduces computational time. Only the first method has been chosen in this project although a comparative study between values obtained by the two methods could be of interest. (Beyond the scope of this Master Thesis).

2.2.2 Impedance measurements

Some acoustic properties of the absorbers placed as suspended ceilings and wall panels in the simulated classroom are measured using a rectangular Kundt's tube according to the ISO 10354 – 2 [37] at DTU.

The surface impedance values are obtained by means of the Transfer-Function Method, which calculates the complex acoustic transfer function between two $\frac{1}{2}$ inch microphones previously calibrated and placed along the tube. Input signals from these microphones are captured with Pulse software and then the surface

impedance values are obtained using Matlab. The remaining required equipment consists of a small loudspeaker attached to the tube and a Brüel & Kjær Fast Fourier Transform Analysing System PULSE. In addition to capturing the input signals and calculating the transfer function, this device generates the noise signals reproduced by the sound source.

Material samples must be carefully cut according to the shape and dimensions of the tube, and placed at the end. The standard sets a minimum of two different samples for each material. For this project, three samples have been used attempting to obtain more accurate impedance estimations. Also, for each sample of material, the microphone positions are interchanged and the measures repeated in order to correct the mismatch between channels.

Knowing the measured transfer function between microphones H_{12}, the reflection factor values and normalized surface impedance are calculated following the equations:

$$R_0 = \frac{H_{12} - H_{inc}}{H_{refl} - H_{12}} e^{jk2l}$$

$$\frac{Z}{\rho c} = \frac{1 + R_0}{1 - R_0} = r + jx$$

where l is the distance between the sample and the further microphone location, and H_{inc} and H_{refl}, the transfer functions for the incident and reflected waves alone.

It is worth noting that these values are only valid for normal incidence. Assuming local reaction, the random incidence absorption coefficients required for the ODEON simulations can be obtained, knowing the normalized surface impedance by:

$$\alpha_{random} = \frac{8r}{r^2 + x^2} \left[1 - \frac{r}{r^2 + x^2} log_e \left((r+1)^2 + x^2 \right) + \frac{r^2 - x^2}{x(r^2 + x^2)} tan^{-1} \left(\frac{x}{r+1} \right) \right]$$

Besides the local reaction assumption limitations, depending on the distance between the microphones s and the diameter of the tube d, the working frequency range is set within:

$$f_l < f < f_u$$

f_l and f_u are the lower and upper limits respectively.

The conditions for f_u are:

$$f_u d < 0.50 c_0$$

$$f_u s < 0.45 c_0$$

f_l is determined by the distance between microphones. This should always exceed 5% of the wavelength corresponding to the lowest frequency of interest.

Knowing the distance between microphones ($s = 0.042$ m) and the diameter of the tube ($d = 0.07$ m) the working frequency range approximately comprises a range which goes from 400 to 2450 Hz, not even covering the entire 500 Hz octave band [353 – 707] Hz nor the 2000 Hz octave band [1414 – 2828] Hz. Thus, only the 1000 Hz octave band [707 – 1414] Hz values can be considered as valid.

Despite these drawbacks, this method is often a quick and simple way to characterize a material without a need for large samples, as required for the reverberant chamber method [34], which characterizes the behaviour of the materials in real situations much more accurately.

The results obtained by means of Transfer-Function Method are shown in Section 3.1 of the current work.

2.3 Room acoustic measurements

The necessary Impulse Response measurements to obtain the acoustical parameters presented in Section 2.1 are carried out at the Ecophon headquarters in Hyllinge, Sweden. Among the wide variety of laboratories that the company owns there, a small rectangular room and a reverberation chamber have been chosen for the realization of this project. The acoustic conditions in the room can be varied by means of the installation of different ceilings, simulating the conditions that can be found in a typical classroom. The dimensions of the room, hereinafter referred to as classroom, are 7.32 m x 7.57 m x 3.50 m, when there is no suspended ceiling installed. The rear wall is temporary, so it could be demolished, thereby increasing the size of the room in order to simulate a typical open-plan office. The classroom has two suspended grids, where different absorbing materials can be

placed, producing room heights of 3.32 m and 2.70 m. The remaining building elements found in the room are four doors, four windows and two ventilation grilles.

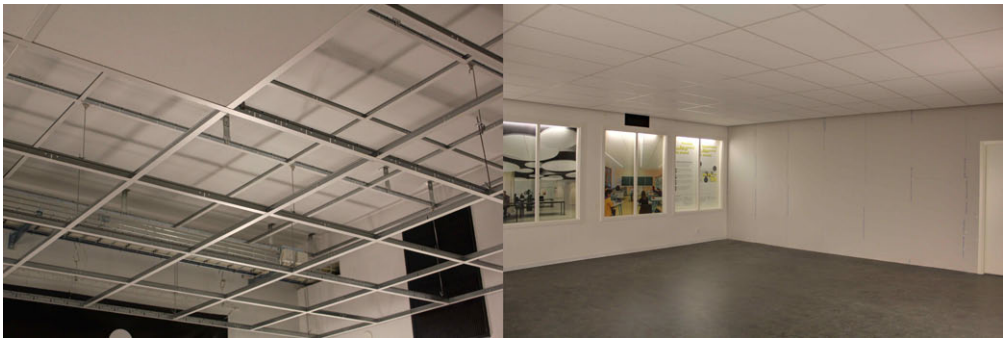

FIGURE 2.1: Recreated classroom in Hyllinge, Sweden

The acoustic materials used for the experiments are porous absorbers produced by the company itself, composed of high density glass wool and placed as suspended ceilings or as wall panels installed on the rear wall of the room. Among the broad range of products manufactured by Ecophon, those used for this work are: Gedina A, Focus A and Industry Modus as ceilings, and Wall Panel C as wall panels. Since each of these materials has a different thickness, for simplicity, hereafter they will be called 15 mm, 20 mm, 50 mm and 40 mm. The dimensions of the plates are also different for each material. They are 0.6 m x 0.6 m for the materials of 15 mm and 20 mm, 1.2 m x 0.6 m for the material of 50 mm, and 2.7 m x 0.6 m for the 40 mm material. Information on the physical properties of the materials is shown in Table 2.2 (with flow resistivity expressed in kPas/m^2 and density in kg/m^3).

Absorber	**Thickness**	**Flow resistivity**	**Density**
Gedina A	15 mm	40	60
Focus A	20 mm	32	55
Industry Modus	50 mm	12	27
Wall Panel C	40 mm	86	100

TABLE 2.2: Physical properties of the absorbing materials

In order to simulate a classroom as realistically as possible, in some of the configurations, 10 typical double desks and 20 chairs are added to the room. The sets of tables and two chairs are placed in 3 rows of 3, while the remaining set, which is for the teacher, is placed in the center at the front of the room. With this arrangement, which can be seen in Figure 2.2, the seating capacity is 18 students and 1 or 2 teachers.

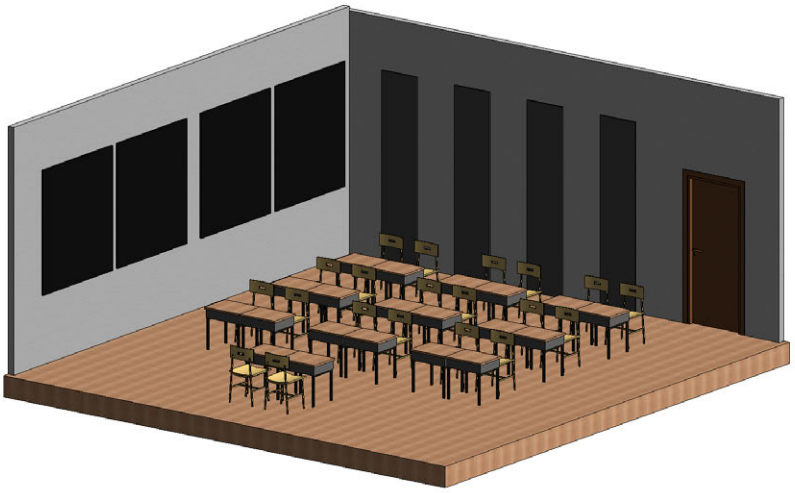

FIGURE 2.2: Furniture distribution

The equipment used to carry out the measures includes:

- Brüel & Kjær omnidirectional sound source Type 4292.
- Brüel & Kjær sound level meter Type 2239.
- Brüel & Kjær USB Audio Interface ZE 0948.
- Brüel & Kjær power amplifier Type 2716.
- Brüel & Kjær sound calibrator Type 4231.
- Laptop with version 4.1.2619 of Brüel & Kjær Dirac software installed.

All this equipment fulfills the normative established in ISO 3382 – 1 [22], ISO 18233 [38], and IEC 61260 [39]. A loudspeaker with a humanlike voice directivity pattern would be desirable, but not mandatory, in order to obtain parameters related to speech intelligibility.

Measurements are made according to the precision method established in ISO 3382 – 2 [23]. This method sets a minimum of 12 different source-microphone position combinations, with at least 2 different source positions. To fulfill these conditions, the measurements of each room configuration are carried out with 2 source positions and 6 microphone positions for each one. The source positions must be chosen according to the use of the room. In this case, considering that the source represents the teacher, it is placed on the teacher's desk and also in a

FIGURE 2.3: Configuration with furniture and wall panels

position between the student desks and the left wall, simulating situations in which the teacher does not remain static throughout a lesson and walks among students. Regarding the microphone positions, these are placed with a separation of at least 2 m between them , 1 m from the nearest reflective surface and 1.50 m from the source, in order to avoid excessive influence of the direct sound. Moreover, the heights chosen for both devices are 1.20 m for microphones, simulating the height of a seated person, and 1.50 m for the source, simulating the height of a standing person. A complete diagram including all source and microphone positions is shown in Figure 2.4.

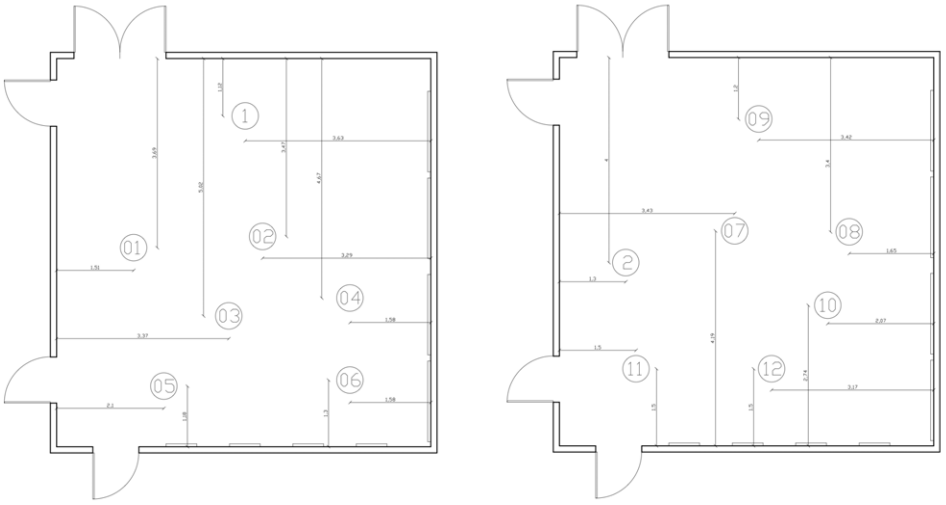

FIGURE 2.4: Source-microphone positions

The procedure chosen for the measurements is the Integrated Impulse Response Method due to the fast speed of implementation when using DIRAC software. The Brüel & Kjær DIRAC Room Acoustics Software Type 7841 is a complete two channels tool for measuring and analysing Impulse Responses. The required excitation signals to obtain the Impulse Responses are directly generated by the software and played through the sound source, simplifying the process and

improving the accuracy of the measurements. Possible excitation signals which can be generated by this software are linear sweeps, logarithmic sweeps and Maximum Length Sequences (MLS). Since MLS sequences excite the entire frequency range at the same time, they are more sensitive to non-linearity and time variance [40]. Therefore, a small change while measuring may affect all frequencies, making the measurements useless. However, sweeps are much more robust to these changes, which only affect the frequency that is being played at the time the change occurs. Besides, the pink frequency spectrum of exponential sweeps can help to improve the Signal-to-Noise Ratio at low frequencies, where the background noise level is usually higher. For these reasons, the exponential sweeps are chosen as an excitation signal.

For most of the measurements, a signal length of 5.46 s is used, except for the configurations without any absorption, where the reverberation time is longer and thus, the length of the excitation signal is increased up to 10.90 s. The frequency range is set to [63 – 8000] Hz and the number of pre-averages is 2. Values of temperature and humidity were more or less constant during all measurements, approximately 18.4 ºC for temperature and 39.3% of relative humidity.

Three different types of calibration are performed before the measurements. First, the set consisting of the sound card, computer and software is calibrated in order to avoid mismatches between them and ensure optimum performance. Subsequently the input level is calibrated using the sound calibrator. To measure Sound Strength, a system calibration is also needed. It is therefore necessary to move the equipment to the reverberation chamber next to the classroom. There, Impulse Response measurements are carried out in 2 different source positions, with 4 microphone positions for each one. Unlike the others, this third calibration can be performed before or after the measurements indistinctly.

Table 2.3 shows all different measured configurations depending on the material used such as ceiling, thickness of the air cavity between the suspended ceiling and the rigid one, the presence of furniture and the wall absorbers. The abbreviated code that identifies each configuration consists of a number, which can be 15, 20 or 50 depending on the thickness of the material used as a ceiling, a letter, which represents the thickness of the air cavity, with A for the thickest and B for the thinnest, and a final part which includes F if the furniture is placed, W in case of placing the wall absorbers and FW if both are present in the room. For configurations where there is no suspended ceiling, the code is simpler, using E for

FIGURE 2.5: System calibration in the reverberation chamber

the empty condition, F for furniture, W for wall absorbers and FW for both. Note that in configuration "20AFe", the microphone and source heights are increased, placing the microphone at a height of 2.33 m and the source at a height of 2.05 m. In configuration "20Af", only one set of desk and chairs is used, in order to better characterize the absorption and scattering produced by these elements.

The most relevant results obtained are shown in Chapter 3 whereas the complete results can be seen in Appendix A.

2.4 Geometrical acoustic simulations

Acoustic simulations of the different situations recreated in Hyllinge are performed using ODEON version 12.12. The ODEON Room Acoustics software is a complete simulation tool originally developed as a cooperation between Danmarks Tekniske Universitet and a number of consulting companies. This software, which in its early version was focused on solving acoustic problems in concert halls, is today one of the reference tools used for the acoustic simulation of any type of room. The calculation of reflections is performed by a Hybrid Reflection Method, which implements the early reflections by using a combination of Image Source and Radiosity methods, and late reflections by a combination of Ray Tracing and Radiosity. Since this is an energy model based on geometric algorithms, phase information is excluded, avoiding interference phenomena and therefore giving erroneous predictions below the cut-off Schroeder frequency. Above this frequency,

Configuration	**Ceiling**	**Air gap** (mm)	**Furniture**	**Wall panels**
20A	20 mm	780		
20AF	20 mm	780	X	
20AFe	20 mm	780	X	
20Af	20 mm	780	X	
15A	15 mm	785		
15AF	15 mm	785	X	
50A	50 mm	750		
50AF	50 mm	750	X	
20AW	20 mm	780		X
20AFW	20 mm	780	X	X
20B	20 mm	160		
20BF	20 mm	160	X	
15B	15 mm	165		
15BF	15 mm	165	X	
50B	50 mm	130		
50BF	50 mm	130	X	
20BW	20 mm	160		X
20BFW	20 mm	160	X	X
E				
F			X	
W				X
FW			X	X

TABLE 2.3: Recreated and measured configurations

the estimation of ISO 3382 acoustical parameters should give completely valid values. Since its last version, ODEON has become a powerful Impulse Response measurement system including internal signal generator. This is an important feature to add to the already existing tools such as auralization, 3D representation of ray tracing and many others.

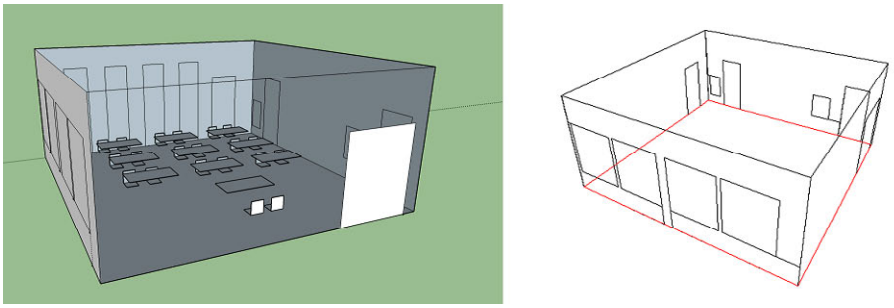

FIGURE 2.6: Room modelled with Sketchup (left) and Odeon (right)

For the implementation of this project, all the different classroom configurations recreated in Hyllinge are modelled by Trimble Sketchup software (version

14). The models are easily incorporated to ODEON using the SU20deon plugin, developed by Odeon and released in 2010.

The surfaces are characterized in ODEON by their octave band absorption coefficients from 63 to 8000 Hz, scattering coefficient, transparency and sound reduction index. The last one is not used for the development of this work. In order to calculate the effect of the scattering, ODEON uses a combined method that takes into account surface roughness and diffraction. A coefficient is assigned by extrapolation or interpolation to each frequency band, based on the scattering coefficient s inputted by the user, which is the value for a frequency around 700 Hz. Values of absorption and scattering coefficients used for modeling the room and furnishings are shown in Table 2.4.

	Absorption coefficient. Frequency (Hz)								
Surface	**63**	**125**	**250**	**500**	**1000**	**2000**	**4000**	**8000**	**s**
Floor	0.01	0.01	0.01	0.01	0.01	0.02	0.02	0.02	0.05
Walls	0.01	0.01	0.01	0.02	0.03	0.05	0.07	0.07	0.05
Ceiling	0.02	0.03	0.04	0.06	0.07	0.08	0.08	0.08	0.05
Temp. wall	0.08	0.08	0.10	0.05	0.02	0.02	0.02	0.02	0.05
Doors	0.17	0.15	0.10	0.04	0.04	0.07	0.08	0.07	0.05
Windows	0.35	0.35	0.13	0.02	0.02	0.02	0.02	0.01	0.05
Grilles	0.60	0.60	0.60	0.40	0.30	0.30	0.30	0.30	0.05
Desks	0.01	0.01	0.03	0.07	0.07	0.08	0.10	0.10	0.50
Chairs	0.25	0.25	0.29	0.29	0.44	0.85	0.90	0.90	0.50

TABLE 2.4: Absorption and scattering coefficients of all surfaces

The floor of the room is a concrete surface, almost totally reflective. The walls and ceiling are made of plaster, the absorption coefficients of which are slightly higher. The temporary wall is made of plaster boards, which present more absorption at low frequencies. Also the wooden doors and windows absorb more at low frequencies since they act as membrane absorbers. The ventilation grilles are quite absorbent surfaces although the effect is not very relevant because they cover a small area. Desks are simulated as wooden panels, with similar coefficients to doors, but lower absorption at low frequencies due to their smaller size and thickness. Each chair is modeled as two rectangular surfaces simulating the seat and backrest. The absorption is high within the entire range of frequencies. It is greater and close to 1 at high frequencies due to the upholstery. Regarding the porous absorbers, extended reaction is assumed for simulations, and absorption coefficients obtained by Miki's Model. Differences between local and extended assumptions when simulating are analyzed in Chapter 4.

The calculation parameters chosen for the simulations are the same for all configurations and according to the Precision setup in ODEON. This sets 2000 as number of early rays, 16000 as number of late rays, and 2000 as maximum reflection order. The transition order is set to 2 and the Impulse Response length to 2000 ms. The angular absorption option is activated to all the surfaces. As there are not many of them, the computational time is not greatly increased. This method, based on the work of Rindel [41], generates angle-dependent absorption coefficients from the values of absorption coefficient introduced by the user, as a function of the incidence angle and size of the surfaces.

The calibration process is performed for configurations E and F, based on reverberation times, T_{20}, simulated and measured for each source position.

CHAPTER 3

Results

3.1 Impedance data

The surface impedance values of the absorbers are obtained by means of the Transfer-Function Method, introduced in Chapter 2. The only material that is found in the simulated classroom under the same conditions as those during the measurements carried out by this method (rigid backing) is the one used as wall panels, the thickness of which is 40 mm.

The surface impedance of the material as a function of the frequency is shown in Figure 3.1.

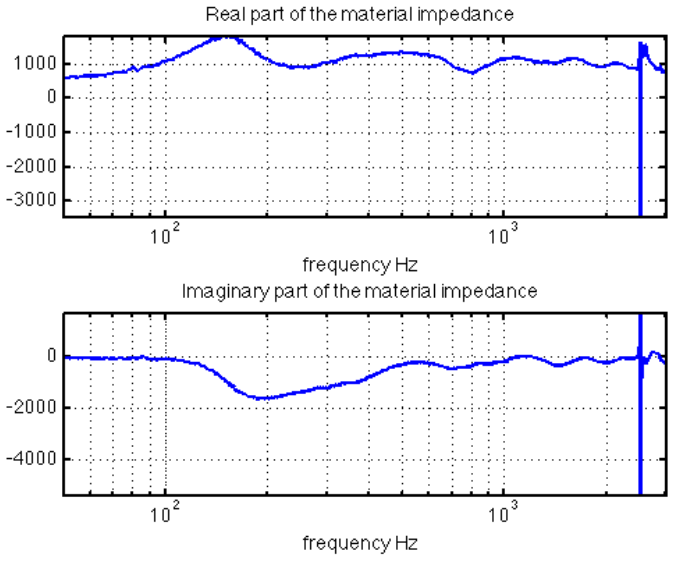

FIGURE 3.1: Real and imaginary part of surface impedance (40 mm)

Note that due to the limited working frequency range of the system, these values can only be considered as reliable between 400 and 2450 Hz.

The surface impedance values and derived random incidence absorption coefficients of all the porous absorbers are shown in Tables 3.1 and 3.2 respectively. Values for frequency bands different to 500, 1000 and 2000 Hz are omitted because of the lack of validity.

	Frequency		
Absorbers	**500 Hz**	**1000 Hz**	**2000 Hz**
15 mm	1947-1628j	699-799j	596-90j
20 mm	1230-1621j	594-630j	591-103j
50 mm	328-654j	287-198j	522-27j
40 mm	1241-457j	1022-193j	993-132j

TABLE 3.1: Octave band surface impedance measured by the Transfer-Function method

	Frequency		
Absorbers	**500 Hz**	**1000 Hz**	**2000 Hz**
15 mm	0.54	0.70	0.94
20 mm	0.51	0.75	0.94
50 mm	0.57	0.78	0.94
40 mm	0.82	0.89	0.90

TABLE 3.2: Octave band random incidence absorption coefficients estimated from surface impedance values

It is important to note that for the 500 and 2000 Hz octave bands, the values cannot be considered as completely valid since some of their frequencies exceed the working frequency range of the system.

Due to the limitations set by the narrow working frequency range and the only possible assumption, which is the local reaction, the values of random incidence absorption coefficient obtained by this method are not included in the simulations.They are only used to compare the results produced by different methods in Chapter 4.

3.2 Parameters

The results of Impulse Response measurements are averaged over the 12 source-microphone combinations for every classroom configuration, in order to obtain a

single value of each acoustical parameter as a function of frequency. In the current Section, only some of the measurement results are shown, whereas the complete results can be viewed in Appendix A.

Once the reverberation time of the room is known, the Schroeder cut-off frequency f_s, given by

$$f_s = 2000\sqrt{\frac{T_{20}}{V}}$$

where V is the volume of the room in cubic meters, is calculated, resulting in a value of about 270 Hz. This frequency is considered as the separation point between low and medium frequencies. Below this value, the modal behaviour of the sound field produces a certain coloration in the frequency response of the room because of the density of eigenfrequencies, which is not high enough within this range. This coloration means that the statistical theories do not give accurate results, since the Impulse Responses are more dependent on the source and microphone positions at these frequencies. This results in a greater dispersion of the results within this range, as shown in Figure 3.2, which shows the results of measured T_{20} for configuration E.

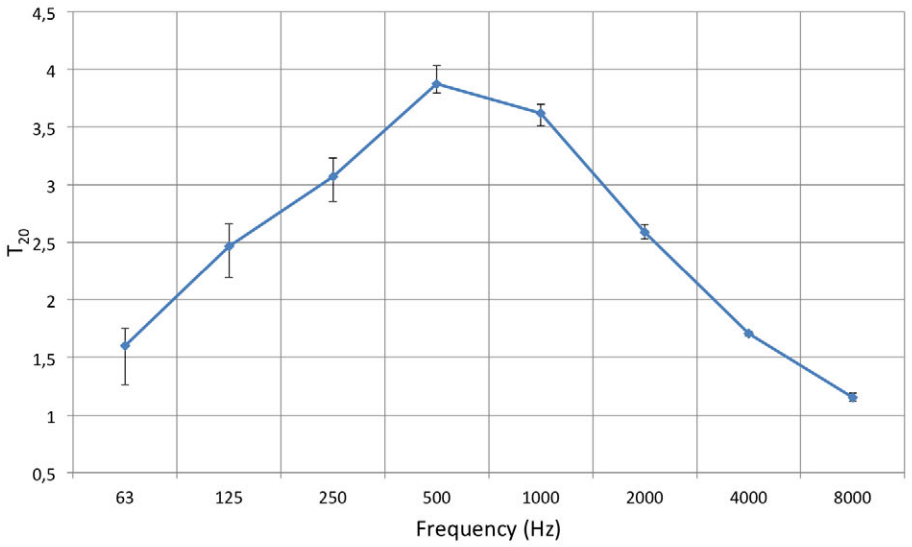

FIGURE 3.2: T_{20} as a function of frequency. Configuration E. No suspended ceiling, no furniture, no wall absorbers

Regarding the acoustic conditions required in classrooms established by the Danish regulation, none of the configurations recreated meet the minimum requirements for reverberation time presented in Chapter 2. It should be noted that, although the additional furniture is a good approximation to the actual furnishings of a classroom as far as the completion of this project is concerned, in

a typical scenario, some other pieces of furniture, such as shelves or lockers, are found. These, in addition to presenting some absorption, act as diffusers, scattering the incident sound energy whenever they are hit by a ray and increasing the absorption produced by the ceiling. This effect, which causes a reduction of reverberation times, is explained in more detail in Chapter 4.

Since the measurements are carried out using an omnidirectional sound source instead of a directive one, the values of STI are not considered as completely valid. Nevertheless, large differences between the results obtained with the two kinds of sources are not expected, so the measured values can be a good estimation of the quality of the speech intelligibility in the room. Based on the classification presented in Chapter 2, under all configurations including furniture and suspended ceiling, the speech intelligibility would be Good. However, in none of the cases it would reach a value of 0.75, which sets the lower limit to an Excellent intelligibility. The best results are obtained for configurations including wall absorbers. The values of T_{20} and STI, measured under the conditions most similar to those that might be found in a real classroom, are shown in Table 3.3.

	Frequency (Hz)								
Conf.	**63**	**125**	**250**	**500**	**1000**	**2000**	**4000**	**8000**	**STI**
20AF	1.28	1.39	1.42	0.80	0.77	0.90	0.89	0.70	0.68
15AF	1.30	1.44	1.51	0.86	0.76	0.88	0.84	0.65	0.69
50AF	1.13	1.03	0.81	0.75	0.82	0.92	0.87	0.71	0.68
20AFW	1.21	1.32	1.23	0.67	0.60	0.65	0.68	0.57	0.74
20BF	1.22	1.24	1.28	0.81	0.86	0.86	0.81	0.64	0.68
15BF	1.22	1.38	1.46	0.81	0.85	0.87	0.83	0.66	0.67
50BF	1.02	0.79	0.81	0.92	0.92	0.91	0.85	0.68	0.67
20BFW	1.15	1.19	1.13	0.65	0.63	0.64	0.62	0.51	0.72

TABLE 3.3: T_{20} and STI measured values under configurations 20AF, 15AF,50AF, 20AFW, 20BF, 15BF, 50BF, 20BFW

Due to the non-existence, or lack of knowledge by the author, of acoustical regulations for classrooms depending on the other measured parameters, conclusions about the quality of the room, based on their values, are not part of this study. However, the acoustic effect produced by placing a suspended ceiling, furniture, or wall absorbers can be relevant. The effect of these elements on the reverberation times is analyzed in detail in Chapter 4.

The variations in C_{50} and G due to the addition of these elements in the classroom can be seen in Figures 3.3 and 3.4 respectively, which show the values

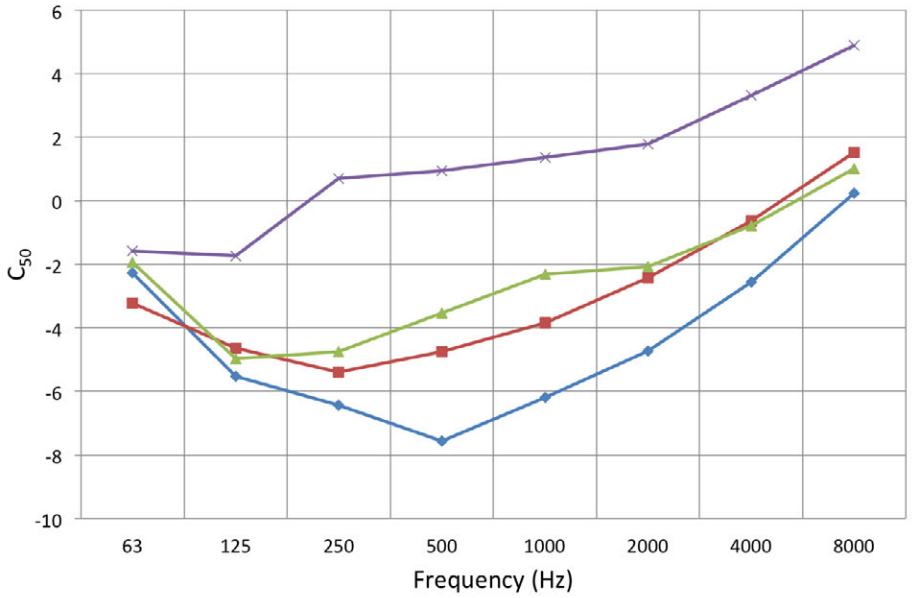

FIGURE 3.3: C_{50} as a function of frequency. Configurations E (blue), F (red), W (green) and 20B (purple)

of these parameters measured for configurations E, F, W and 20B, as a function of frequency.

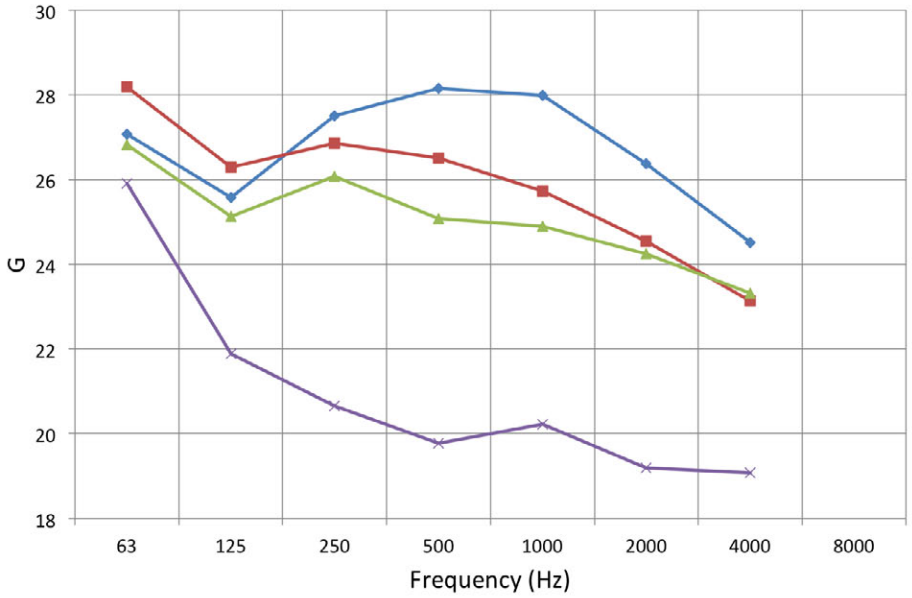

FIGURE 3.4: G as a function of frequency. Configurations E (blue), F (red), W (green) and 20B (purple)

As expected, for both C_{50} and G, the greatest effect is produced by the installation of the suspended ceiling, in this case, the 20 mm material backed by a 160

mm air cavity. Also, for both parameters, the wall absorbers produce a greater variation than desks and chairs.

3.3 Simulations

The results of the calibration procedure and the most relevant simulations are shown in this Section. In addition, the complete results of simulation, presented as comparative graphs between measured and simulated T_{20} for each classroom configuration can be viewed in Appendix B.

The calibration between simulated and measured reverberation times is carried out carefully, in order to obtain reliable simulation results. Firstly, absorption coefficients of the building elements are chosen for configuration E, so as to avoid discrepancies between measured and simulated values. Realistic values must be chosen if the goal of the simulations is to draw accurate conclusions. Once the values have been selected, the process is repeated for configuration F in order to also calibrate the absorption coefficients of desks and chairs. Calibration results of both configurations are shown in Figure 3.5.

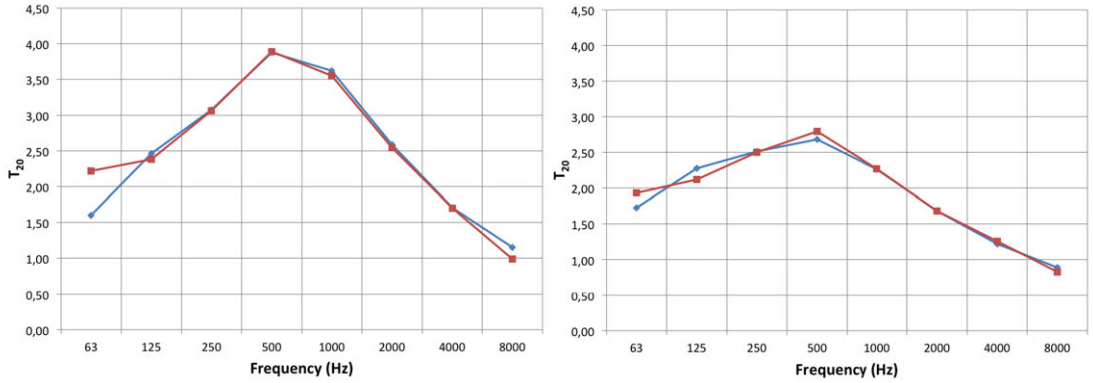

FIGURE 3.5: Simulated versus measured T_{20} as a function of frequency. Configurations E (left) and F (right). Simulations in red, measurements in blue

As can be seen in both graphs, large differences are avoided, except for those found in the octave band the central frequency of which is 63 Hz. Here, the results are not valid due to the modal behaviour of the room below the cut-off Schroeder frequency. Note that the absorption coefficients of the chairs used for a correct calibration of the model are likely higher than the actual ones, in order to correct the increase of absorption produced by the diffraction effect, presented in Section 2.2.

The diffraction effect, also called edge effect, can produce large discrepancies between measurements and simulations, since ODEON does not take it into account when implementing its estimations. A good example of these huge discrepancies can be seen in Figure 3.6, which shows the difference between T_{20} measured and simulated values for configuration W.

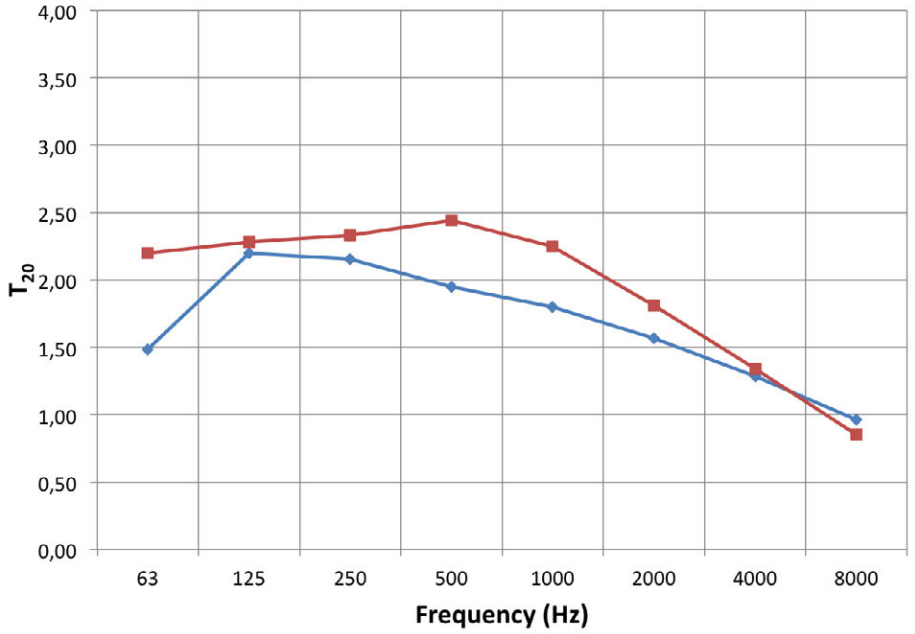

FIGURE 3.6: Simulated versus measured T_{20} as a function of frequency. Configuration W with no corrections. Simulations in red, measurements in blue

It should be kept in mind that these large discrepancies are not only due to the edge effect, but are also produced by the difference between the actual absorption area of the wall panels and its modeled area. When modeling a room to be incorporated to ODEON, all surfaces with a smaller length than a middle frequency wavelength (about 30 cm) should be avoided, because they may cause undesirable results. For that reason, the wall panels with a thickness of 40 mm are modeled as planar surfaces omitting their thickness, and therefore a part of the absorbing surface exposed to sound incidence is excluded. In situations where the modeled area is much larger than the area due to the depth of the material, this effect has no relevance. This is not the case found in the configurations studied in this work, where the area of the edges represents 15% of the total area and therefore can not be omitted. Both effects, which may cause large discrepancies, can be corrected in order to obtain simulation results which are as realistic as possible . Size correction of the absorbers is made with two different methods that give very similar results. The first method (absorption coefficient thickness

correction) consists in multiplying the absorption coefficients of the material by a factor which is proportional to the percentage of the total area represented by the area of the edges. The results of this calculation are new absorption coefficient values, which are completely valid for incorporation into the model, where the wall panels are modeled as planar surfaces. Thus, 15% percent of the area involving the edges is added by simply changing the absorption coefficient values and without changing the entire model. The absorption coefficients of the wall panels (40 mm) before and after correction are shown in Table 3.4.

	Frequency (Hz)							
Abs. coef.	**63**	**125**	**250**	**500**	**1000**	**2000**	**4000**	**8000**
α_{Miki}	0.08	0.21	0.43	0.65	0.78	0.85	0.90	0.93
$\alpha_{corrected}$	0.09	0.24	0.49	0.74	0.89	0.97	1.03	1.06

TABLE 3.4: Absorption coefficient values (40 mm), with and without absorption coefficient thickness correction

As shown, in some octave bands (4000 and 8000 Hz), the values of absorption coefficients exceed unity. They are not therefore valid values for incorporation into ODEON, which is not able to simulate the behaviour of materials with absorption coefficients greater than 1. For that reason, this correction method is discarded as opposed to the second method, which requires modification of the model.

The second method (size correction) consists in adding the area due to the depth of the material as a part of the planar surfaces that represent the wall panels when modeling. Thus, the total area exposed to sound incidence in the model is increased by 15% and therefore matched to the total area exposed in the actual scenario, so that the absorption coefficient values obtained by Miki's Model can be directly applied, since none of them exceeds unity. The results obtained using each correction method are compared with the measured T_{20} values in Figure 3.7. Henceforth, this second method will be used in all simulations involving wall panels.

Corrections to counteract the effect of the diffraction are more complicated, since in most cases, the absorption coefficients obtained as a result of the process are greater than unity. The procedure (absorption coefficient diffraction correction) is based on the method for the measurement of sound absorption in a reverberation chamber established in ISO 354 [34]. Since the size of the samples and the conditions of diffusion in the room do not comply with the principles set out in that standard, this method is explained here but it is not incorporated into the

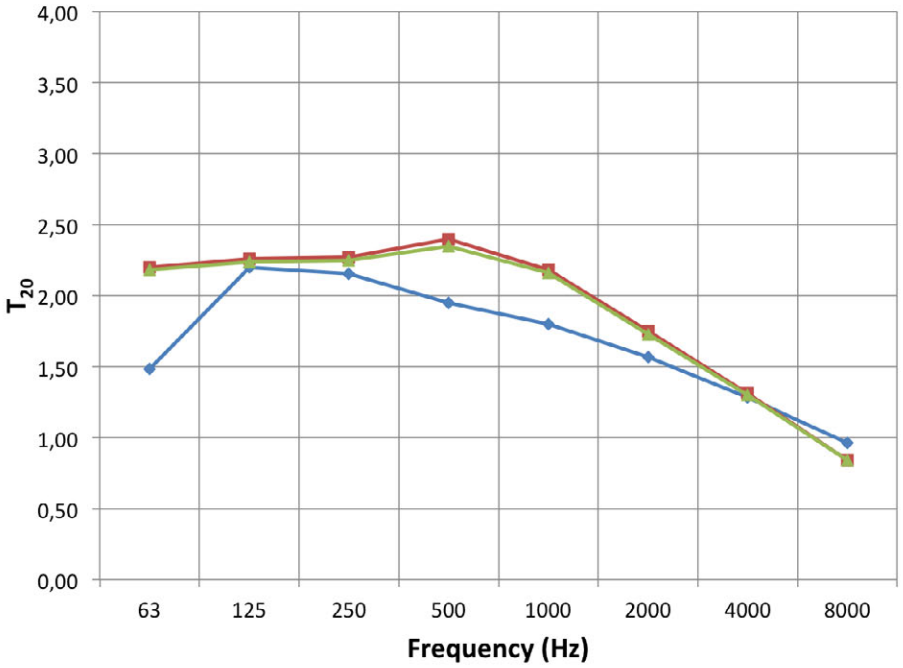

FIGURE 3.7: Simulated versus measured T_{20} as a function of frequency for configuration W. Simulated with absorption coefficient thickness correction in green, simulated with size correction in red, and measured in blue

simulations. It must also be taken into account that this method is applicable to this project because of the large amount of available data about reverberation times of the room when the material is included and when it is not. This however is not usually common in acoustic projects, in which normally the measurements are made with several different elements in the room. Then it is complicated to characterize the effect of only one element.

The method involves the characterization of the effect produced on reverberation times by placing an absorber in a reverberant room. Such an effect results in new absorption coefficient values, which take the diffraction effect into account.

The equivalent sound absorption area of the material A_T, in square meters, is given by:

$$A_T = \frac{55,3V}{c}\left(\frac{1}{T_2} - \frac{1}{T_1}\right)$$

where c is the propagation speed of sound in air, V is the volume of the room, T_1 the reverberation time of the empty room and T_2 the reverberation time when the material is placed in the room. Note that, for simplicity, the attenuation caused by the air has not been taken into account.

Knowing the values of A_T for each frequency band, the absorption coefficients are calculated by using:

$$\alpha = \frac{A_T}{S}$$

where S is the total area of the introduced samples. The absorption coefficients obtained are shown in Table 3.5.

	Frequency (Hz)							
Abs. coef.	**63**	**125**	**250**	**500**	**1000**	**2000**	**4000**	**8000**
α_{354}	0.21	0.21	0.58	1.16	1.17	1.05	0.80	0.71

TABLE 3.5: Absorption coefficient values (40 mm) obtained by the reverberation room method

As can be seen, some of the absorption coefficient values exceed unity, and therefore are not suitable for incorporation into the simulations. As an illustrative example, and with no validity, values greater than 1 are truncated and applied in the simulations. Figure 3.8 shows a comparison between values of T_{20} measured and simulated, with and without applying the absorption coefficient diffraction correction. Hereafter, only the size correction will be applied to simulations.

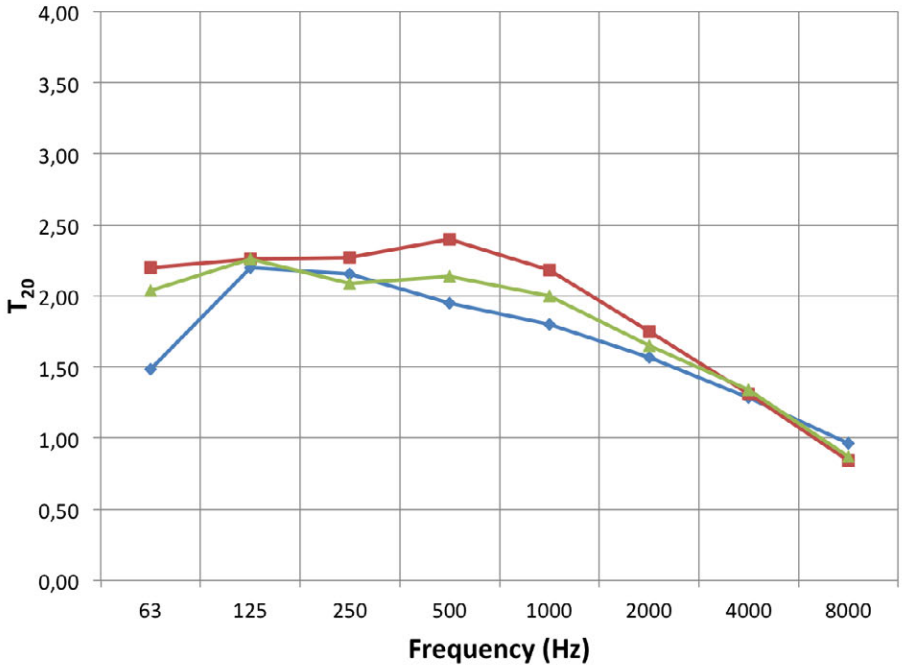

FIGURE 3.8: Simulated versus measured T_{20} as a function of frequency for configuration W. Simulated with size and absorption coefficient diffraction correction in green, simulated with size correction in red, and measured in blue

The simulation results obtained for all the situations are quite consistent, especially above the cut-off Schroeder frequency. Figure 3.9 shows how ODEON simulates the effect caused on reverberation times with the introduction of a suspended ceiling, furniture and wall panels into the room.

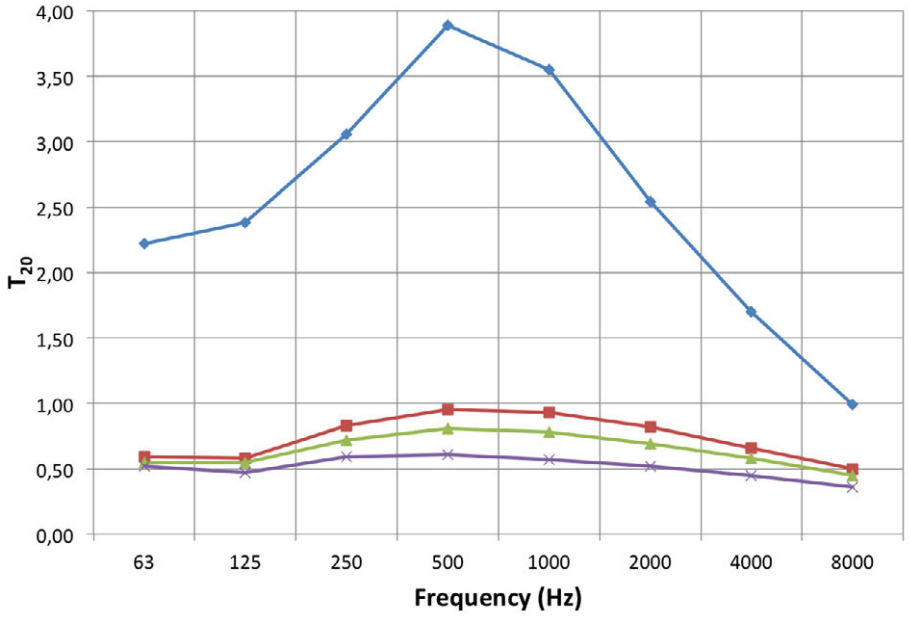

FIGURE 3.9: Simulated T_{20} as a function of frequency for configurations E (blue), 20A (red), 20AF (green) and 20AFW (purple)

However, large discrepancies are found between the simulated and measured values of T_{20} for almost all the configurations. Possible reasons for these discrepancies are discussed in Chapter 4.

CHAPTER 4

Analysis and discussion

4.1 Non-diffuse sound field

Based on the work by Erling Nilsson [42], the decay curves obtained from the measured Impulse Responses are analyzed. It is well known that Sabine's equation works quite well with diffuse sound fields. However, under non-diffuse conditions, such as those usually found in classrooms, the predictions calculated by using this formula do not often achieve a high degree of accuracy. The diffusion in a room is determined by its shape and the acoustic characteristics of its surfaces. The distribution of absorbers and the amount of scatter objects and surfaces are key factors for a diffuse sound field. The decay curves, therefore, are also influenced by these characteristics, showing different slopes depending on the materials placed in the classroom. When the sound field in a room is completely diffuse, the sound pressure level drop is uniform. It is represented by a straight line as the decay curve. The decay curve at 2000 Hz for configuration E, measured and calculated according to Sabine's equation is shown in Figure 4.1. The graph has been truncated in order to show only the first 30 ms, as these are the most relevant for this study. It can be seen how the decay curve essentially follows a straight line, very similar to the one calculated by Sabine's equation. This indicates that the sound field in this configuration is close to diffuse.

If the dimensions of the room are modified and absorbing materials introduced, the decay curves do not follow a straight line, showing some changes of slope. This is the case of configuration 20B, in which the height of the room is decreased and the amount of absorption increased by the introduction of a suspended ceiling.

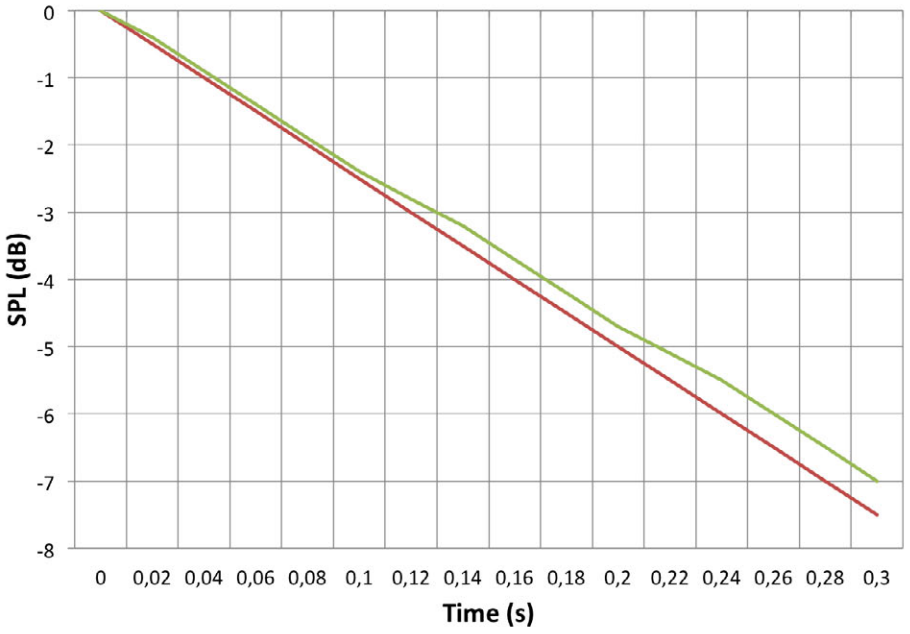

FIGURE 4.1: Decay curves at 2000 Hz, measured (green), and calculated by Sabine's equation (red). Configuration E

Decay curves at 2000 Hz, measured and simulated with Sabine's equation for this configuration, are shown in Figure 4.2.

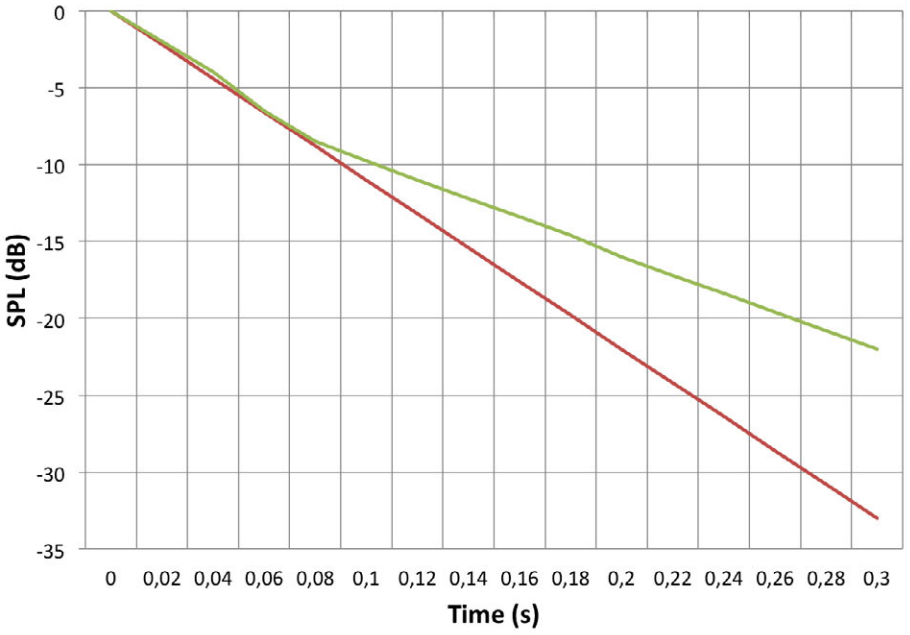

FIGURE 4.2: Decay curves at 2000 Hz, measured (green), and calculated by Sabine's equation (red). Configuration 20B

The former part of the measured curve nearly follows the same path as that calculated by Sabine's equation. A change of slope is observed, followed by a

final part, which tends to increase the difference to the simulated curve. This means that the behaviour of the sound field is far from diffuse. Nilsson explains this by the division of the sound field into two different components, one grazing, comprising waves traveling parallel or nearly parallel to the absorbing surface, hitting it from large angles of incidence with respect to the perpendicular direction to the absorber, and a non grazing component, comprising the rest of the sound waves. The influence of non grazing waves is represented by the first part of the decay curve, the fall of which is usually steeper, due to the higher absorption presented by the material when it is hit perpendicularly or almost perpendicularly. The grazing component determines the final part of the curve, which drops more slowly, due to the low absorption presented by the material when it is hit with small angles of incidence.

In rooms that have a diffuse sound field, the introduction of scattering objects does not produce a noticeable effect. However, under non-diffuse conditions, such as found in some of the simulated configurations, the introduction of scattering elements, such as desks and chairs, may produce huge changes. The scatters cause an exchange of energy from the grazing to the non grazing field [43], since the sound energy is scattered when they are hit, and waves that were traveling parallel to the absorber start traveling in multiple directions, hitting the ceiling and being absorbed by it.

So far, the effect of the introduction of highly absorbent materials and furnishings has only been analyzed from the point of view of the changes produced in the decay curves and their relationship to the more or less diffuse behaviour of the sound field. Due to the slope changes found in the decay curves, the reverberation time varies depending on the section of the curve chosen to calculate it. As has been explained previously in this paper, to calculate EDT, the first part of the curve, comprising a 10 dB drop is used, while for the calculation of T_{20}, the section is chosen from at least 5 dB below the steady state sound pressure level. These differences are not significant in cases where the decay curves follow a straight path. However, large discrepancies are found between the different parameters that characterize the reverberation time when the sound field is far from diffuse. The different values of the reverberance descriptors obtained from the measured Impulse Responses are compared to the reverberation time calculated according to Sabine's equation for configuration E in Table 4.1.

	Frequency (Hz)							
Reverb. time	**63**	**125**	**250**	**500**	**1000**	**2000**	**4000**	**8000**
EDT	1,12	1,98	2,91	3,87	3,58	2,48	1,67	1,05
$\mathbf{T}_{20}$	1,3	2,42	3,05	3,88	3,61	2,59	1,70	1,09
$\mathbf{T}_{sabine}$	3,00	1,87	3,18	3,88	3,54	2,54	1,71	0,99

TABLE 4.1: Values of reverberation time measured and calculated by Sabine's equation. Configuration E

Except for frequencies below the Schroeder cut-off frequency, where the Impulse Responses are more dependent on the microphone and source positions and thus generalized conclusions can not be drawn, the values of EDT, T_{20} and T calculated by Sabine's equation, T_{sabine}, are quite similar. The differences are no larger than 10% of their value. This indicates again that under these conditions the sound field is quite diffuse since in a theoretical diffuse sound field, reverberation times calculated by all the different methods should be equal. The different reverberation times for configurations 50A and 50AF are shown in Figure 4.3. In both cases, the differences are larger than those obtained under configuration E. This means that the resulting sound fields are far from diffuse. The effect of the introduction of furniture, which reduces the differences due to the scattering increase, can also be seen.

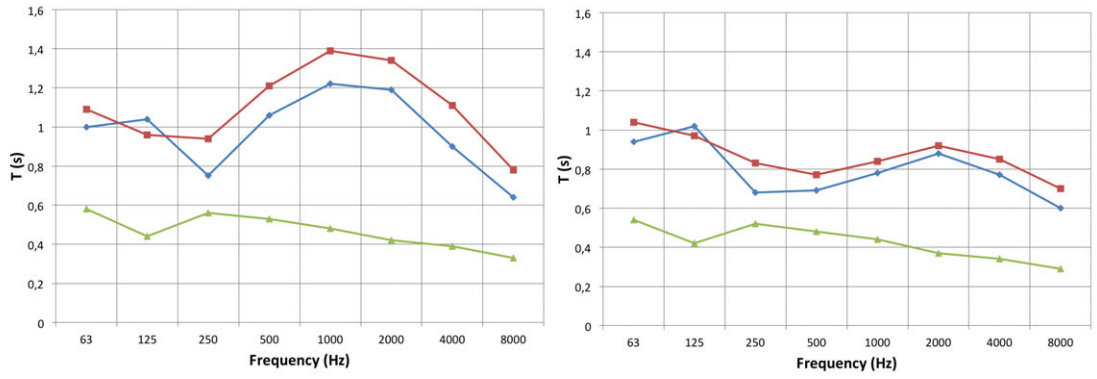

FIGURE 4.3: Different reverberation times as a function of frequency. EDT in blue, T_{20} in red and T_{sabine} in green. Configurations 50A (left) and 50AF (right)

4.2 Impedances and absorption coefficients

The absorption coefficient values of the absorbers obtained by the different methods previously explained and the effect caused on the reverberation times are

analyzed in this Section. The measurements in Hyllinge are taken as reference and compared with the simulation results obtained using the different values of absorption coefficients. Absorption coefficients obtained by the impedance tube method are not applied to the simulations, because of its limited operation range and the large discrepancies found with the values obtained by other methods.

Values of random incidence absorption coefficients of the 40 mm material backed on a rigid surface measured in a Kundt's tube, measured by the reverberation chamber method (extracted from Ecophon website) and estimated by Miki's Model, are compared in Figure 4.4.

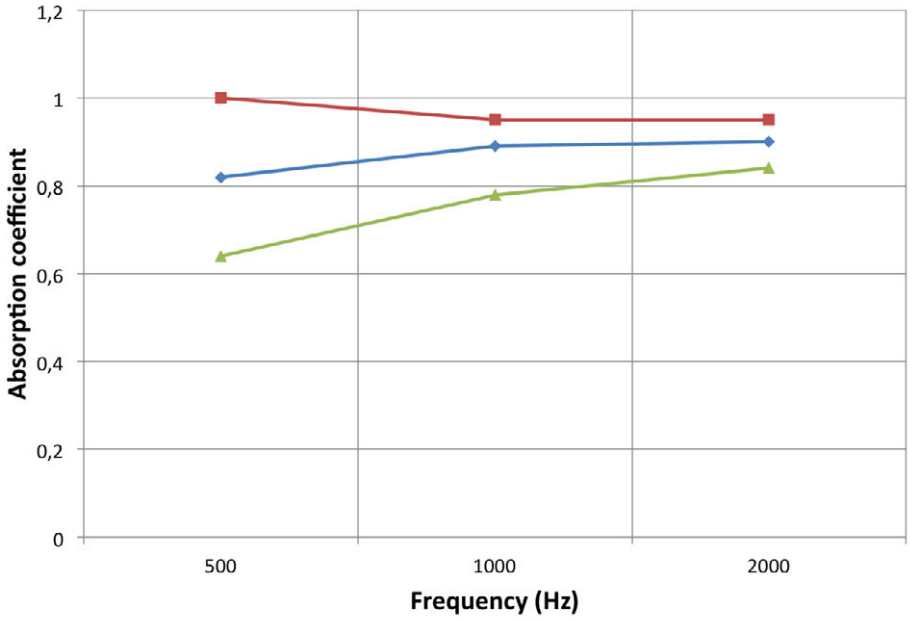

FIGURE 4.4: Absorption coefficients of 40 mm absorber measured by the impedance tube (blue) and reverberation chamber (red) methods, and estimated by Miki's Model (green)

The results are limited to the octave bands centered at 500, 1000 and 2000 Hz due to the valid frequency range of the impedance tube method. Local reaction is assumed for this method as well as for the estimations obtained by Miki's Model. The differences found between the values obtained by the reverberation chamber method can be explained by diffraction, the effect of which always produces absorption coefficient values higher than the actual ones. The differences found between values measured in the tube and those estimated, fit the conclusions drawn by Jeong [35], who compares the random incidence absorption coefficients obtained by different methods, reaching the conclusion that local reaction always underestimates the actual values for rigid backing.

In addition, a better correlation between the values measured in the tube and the estimations using Miki's Model is observed when the thickness of the material increases. It has not been possible to establish a valid relationship between them due to the very limited number of experiments carried out.

Random incidence absorption coefficients estimated by Miki's Model of the three materials placed as suspended ceiling are compared, in order to find a relationship between their physical properties and the amount of absorption produced. Since each of these materials is backed by an air cavity of varying thickness, a fixed value of 160 mm is chosen for this comparison. In addition, extended reaction is assumed. The author considers that this provides a better model of the behaviour of materials, when they are backed by an air cavity. The values of random incidence absorption coefficients obtained following the patterns explained above are shown in Table 4.2.

	Frequency (Hz)							
Absorber	**63**	**125**	**250**	**500**	**1000**	**2000**	**4000**	**8000**
15 mm	0,09	0,26	0,57	0,83	0,70	0,80	0,87	0,94
20 mm	0,10	0,29	0,61	0,85	0,73	0,84	0,91	0,95
50 mm	0,16	0,42	0,74	0,88	0,84	0,93	0,95	0,96

TABLE 4.2: Absorption coefficients of all the ceiling materials obtained by Miki's Model assuming extended reaction

Since the flow resistivity and density of these materials decrease as the thickness increases, it is difficult to establish relationships between those parameters and the amount of absorption. The only certainty is that the absorption coefficients increase with the thickness, mainly at low frequencies. In order to check the validity of Miki's Model in such configurations, the effect on measured reverberation times caused by the introduction of the three materials into the room is compared in Figure 4.5. Note that the thickness of the air cavities varies slightly in the simulated configurations from the value of 160 mm previously set as reference. The established relationship between thickness and absorption must now be questioned in the light of the effect on reverberation times, especially at high frequencies, where the thinnest materials produce shorter reverberation times. Since the valid operation range of Miki's Model contains almost all the frequency bands compared here, as well as the area of material, which is the same and is placed in the same position for all three configurations, it appears that this unexpected effect may be due to the angle-dependent behaviour of these porous absorbers.

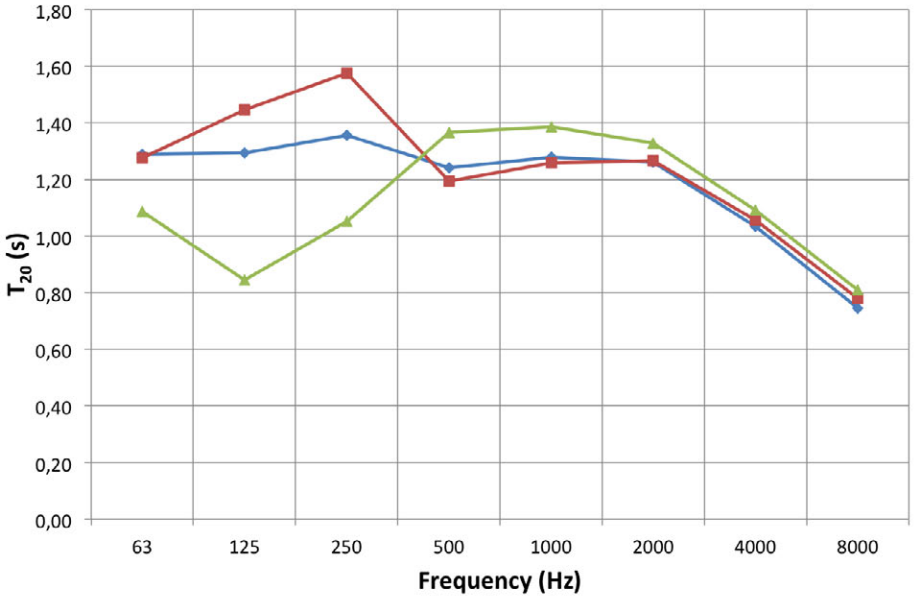

FIGURE 4.5: Measured T_{20} as a function of frequency for configurations 20B (blue), 15B (red) and 50B (green)

Since the room sound field is far from diffuse when the suspended ceiling is placed, the probability of incidence of a sound wave on the absorber is different for each angle. Therefore, the random incidence absorption coefficient is not a good descriptor of the absorption caused by the material in these cases. The absorption coefficients obtained by Miki's Model for the 20 mm and 50 mm materials backed by air cavities of 160 and 130 mm, respectively, are shown as a function of incidence angle in Figure 4.6. Extended reaction is assumed.

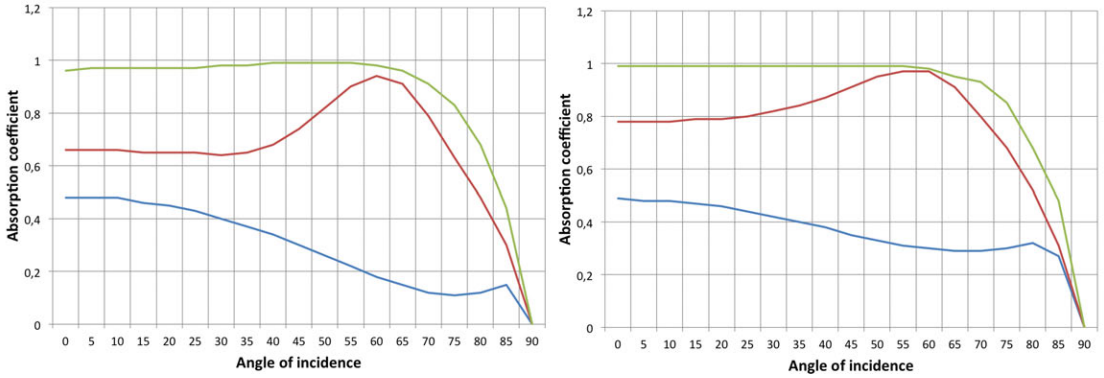

FIGURE 4.6: Absorption coefficient as a function of incidence angle at 125 Hz (blue), 1000 Hz (red) and 8000 Hz (green). 20 mm ceiling (left) and 50 mm ceiling (right)

As can be seen, the angle-dependent behaviour varies for each material. The absorption maxima changes with the angle and this makes it much more difficult

to find relationships between the physical properties of the materials (thickness, density and flow resistivity) and the amount of absorption produced. The largest variations with respect to the horizontal line which would represent the theoretical behaviour of the absorption coefficient are found for angles relating to the grazing component of the sound field. This, coupled with the fact that in such rooms the sound waves tend to hit the absorber from these angles [1], explains that longer reverberation times can be achieved with materials which have higher random incidence absorption coefficients.

Furthermore, assuming local or extended reaction is decisive when modeling the angle-dependent behaviour of the material, as confirmed in Figure 4.7, which shows the difference between the estimated values of absorption coefficient of the 15mm material at 1000 Hz, assuming both reactions.

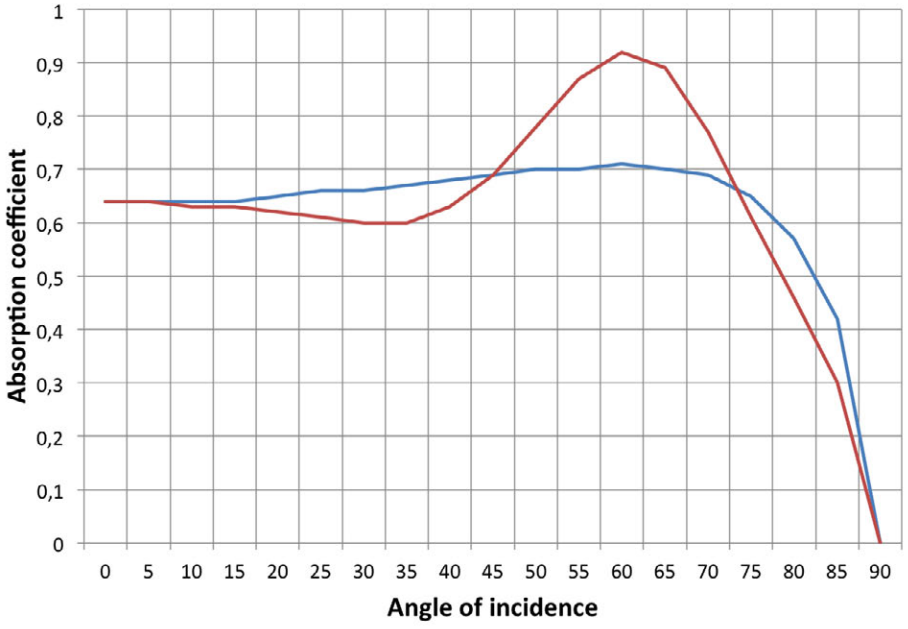

FIGURE 4.7: Absorption coefficient as a function of incidence angle. Local reaction in blue and extended in red

The values of absorption coefficient obtained by Miki's Model are also different when assuming local or extended reactions. The differences in random incidence absorption coefficients are very similar for the three materials used. The thinner the air cavity, the greater the differences. Table 4.3 shows the absorption coefficients of the 15 mm material backed by an air cavity of 165 mm, obtained by Miki's Model assuming both reactions, local and extended. The variations follow the same pattern for the three materials, differing considerably at low frequencies and having higher absorption when assuming local reaction, whereas at high

	Frequency (Hz)							
Reaction	**63**	**125**	**250**	**500**	**1000**	**2000**	**4000**	**8000**
Local	0,27	0,55	0,82	0,92	0,67	0,82	0,84	0,89
Extended	0,10	0,27	0,58	0,83	0,70	0,80	0,87	0,94

TABLE 4.3: Absorption coefficients obtained by Miki's Model assuming local and extended reactions. 15 mm ceiling

frequencies the differences are smaller and more absorption is achieved when the extended reaction is assumed. The effect on reverberation time when the materials are modeled under both assumptions is also relevant to deciding which of these reactions better models the actual behaviour of the absorbers. Figure 4.8 compares the measured and simulated reverberation times as a function of frequency for configuration 15B. Again, the coefficients obtained by means of the

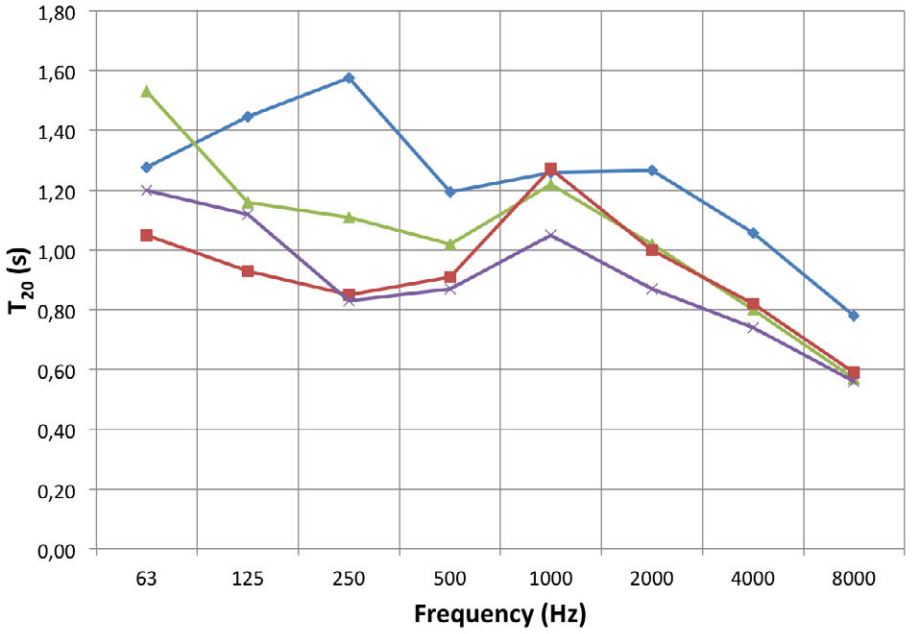

FIGURE 4.8: Reverberation times measured (blue), simulated assuming extended (green) and local (red) reactions, and simulated with ISO 354 coefficients (purple) for configuration 15B

reverberation chamber method [34] overestimate the absorption. It is important to note that the ISO 354 coefficients taken from the Ecophon datasheet have been measured for a total depth of the system of 200 mm, and then the values may vary slightly. Also, an overestimation is observed in most frequency bands when the absorbers are modeled with the coefficients obtained by Miki's Model assuming either of the reactions. This is due to the simulations with ODEON, which does not model accurately the angle-dependent behaviour of the materials. Despite

this, a better correlation between the values obtained assuming extended reaction at low frequencies (where simulation results are more questionable) is observed, while the local reaction works slightly better at high frequencies. In configurations including furniture, where the sound field is more diffuse, the results are similar, showing that there is no relationship between the degree of diffusion and the reaction assumed. However, in these cases, simulations seem to agree better with the measured values. This can be seen in Figure 4.9, which shows the measured and simulated reverberation times for configuration 15BF.

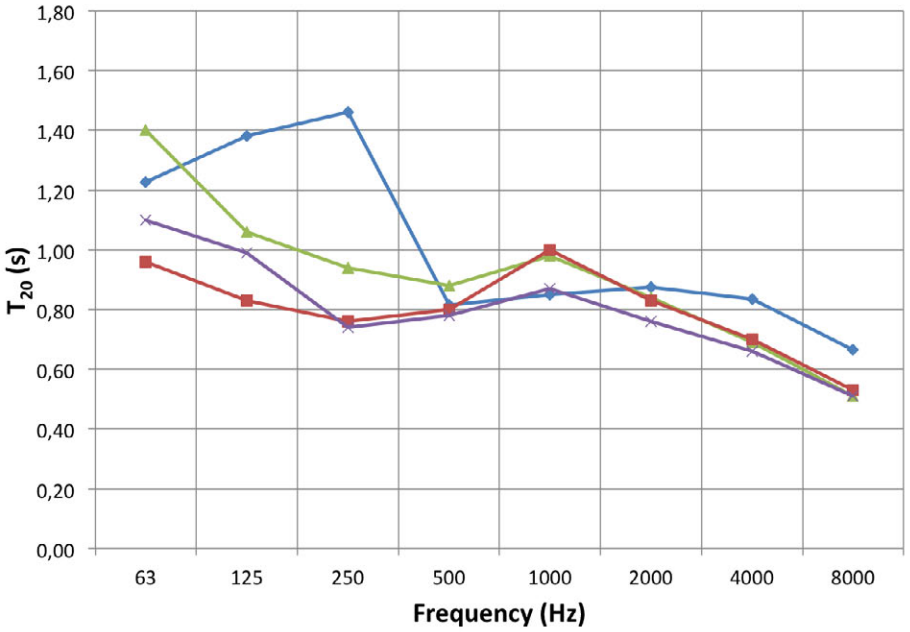

FIGURE 4.9: Reverberation times measured (blue), simulated assuming extended (green) and local (red) reactions, and simulated with ISO 354 coefficients (purple) for configuration 15BF

4.3 Measurements

The results of the measurements carried out in Hyllinge, mostly reflect the acoustical behaviour expected, although some inconsistencies have been found. These are discussed below.

The introduction of furniture, as expected, causes a reduction in reverberation times because of the absorbing properties of desks and chairs and the scattering produced. As explained above, this scattering leads to an energy exchange between grazing and non grazing sound field components. Consequently, the suspended

ceiling offers a better performance. This effect can be seen in Figure 4.10, which compares the reverberation time T_{20} measured for configurations 20A, 20Af and 20AF.

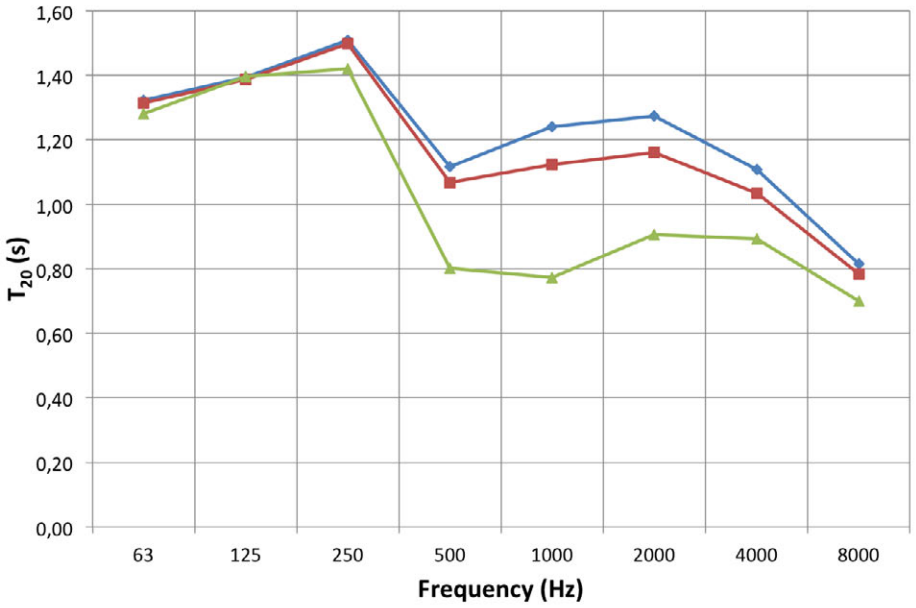

FIGURE 4.10: T_{20} as a function of frequency. Configurations 20A (blue), 20Af (red) and 20AF (green)

The decrease is more evident at high frequencies due to the higher absorption of the chairs within this range. Since the degree of diffusion at low frequencies is high for all configurations, the introduction of furniture does not produce significant changes in the sound field. The effect of the wall panels is also as expected. They reduce reverberation times throughout the bandwidth, although mainly at high frequencies. Reverberation times for configurations E, W, 20A and 20AW are shown in Figure 4.11. This demonstrates how the introduction of wall panels in the empty room produces a considerable decrease in reverberation times. Logically, the decrease resulting from the introduction of the suspended ceiling is the highest, due to the much larger amount of material. Placing both elements simultaneously gives the most effective results. Reverberation times are close to the required values although the absorption at low frequencies is still far from desirable. The placement of the same materials as a suspended ceiling backed by air cavities of different thicknesses is what produces the most unexpected results. While the expected behaviour would be an increase of absorption at low frequencies coupled with a lower absorption at high frequencies when the air cavity is thicker, the effect produced is the opposite. This can be seen in Figure 4.12, which shows the reverberation times measured for configurations 15A, 15B, 15AF and 15BF. Both

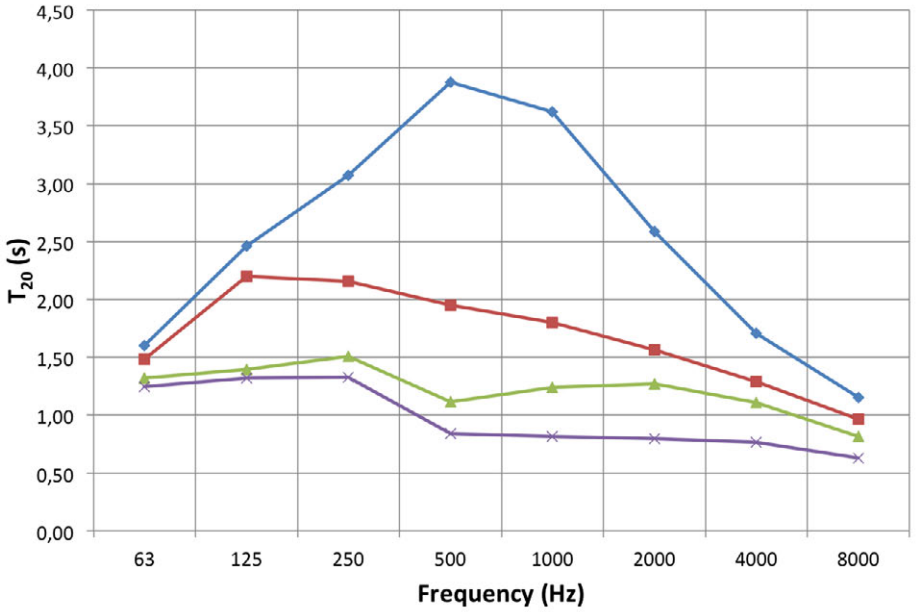

FIGURE 4.11: T_{20} as a function of frequency. Configurations E (blue), W (red), 20A (green) and 20AW (purple)

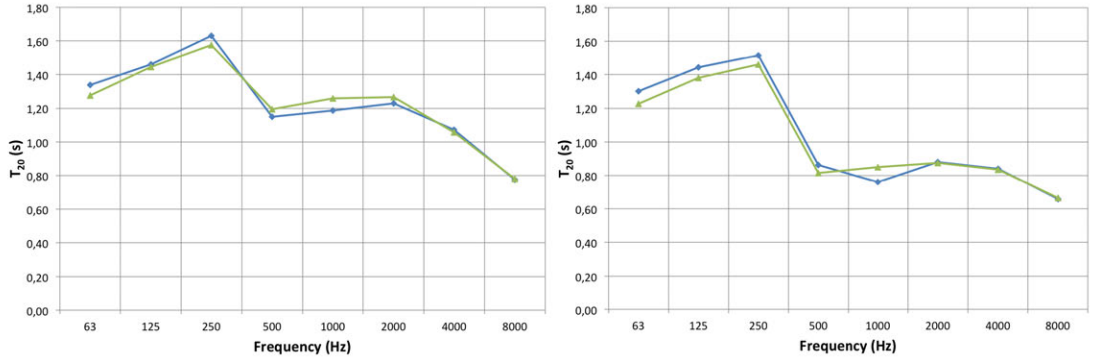

FIGURE 4.12: T_{20} as a function of frequency for configurations 15A (blue) and 15B (green), without (left) and with furniture (right)

in configurations including only the suspended ceiling and in those including also furniture, the tendency is the same. We see longer reverberation times at low frequencies and shorter or similar times at high frequencies when the air cavity is thicker. The same pattern is followed with all three materials. This unexpected effect, which implies higher absorptions for materials with lower random incidence absorption coefficients, can also be explained by the angle-dependent behaviour of the materials. Figure 4.13 shows the absorption coefficient versus the angle of incidence of the material with a thickness of 15 mm, backed by air cavities of 165 mm and 785 mm at 2000 Hz. Depending on the thickness of the air cavity, we see that the absorptions are higher for certain angles of incidence and lower for others. If most of the sound waves at that frequency hit the absorber from

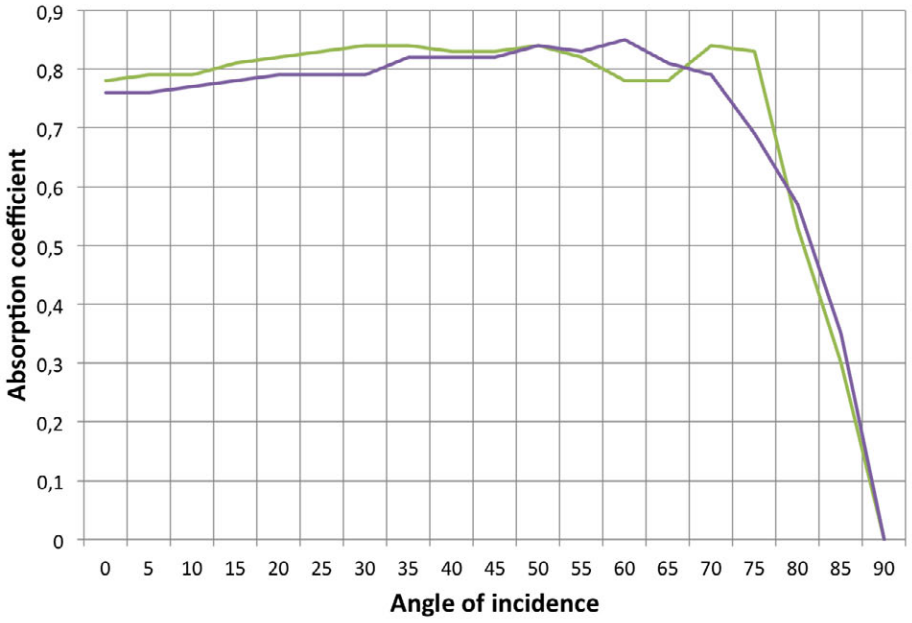

FIGURE 4.13: Absorption coefficient as a function of incidence angle. 15 mm material backed by an air cavity of 165 mm (green) and 785 mm (purple)

an angle in which the absorption produced by the system formed by the material and the cavity is lower, longer reverberation times will be obtained, although the values of random incidence absorption coefficient of the system are higher and vice versa. Furthermore, the increase in the thickness of the air cavity results in a decrease in the height of the room, which will give it a more irregular shape. This usually involves a more directional sound field. As has been explained above, a more directional sound field is more dependent on the angle-dependent behaviour of the materials, and this leads to results such as those found in this work, which are difficult to predict using statistical theories. Figure 4.14 shows the absorption coefficients of the material of 15 mm at 250 Hz for large angles of incidence relative to the direction perpendicular to the absorber, for air cavities of 165 mm and 785 mm. It can be observed that, from a given angle, the absorption is the same and it decreases for both cavities. If in the case of the largest cavity, where the sound field is more directional, the sound waves hit the absorber from larger angles of incidence, the absorption coefficients of the system will be lower than those for the configuration with the thinner air cavity. Under this latter configuration, shorter reverberation times are achieved, despite of having lower random incidence absorption coefficients. Since no information about the angles of incidence is available for the cases measured, no definite conclusions can be drawn.

The differences produced in reverberation times depending on the thickness

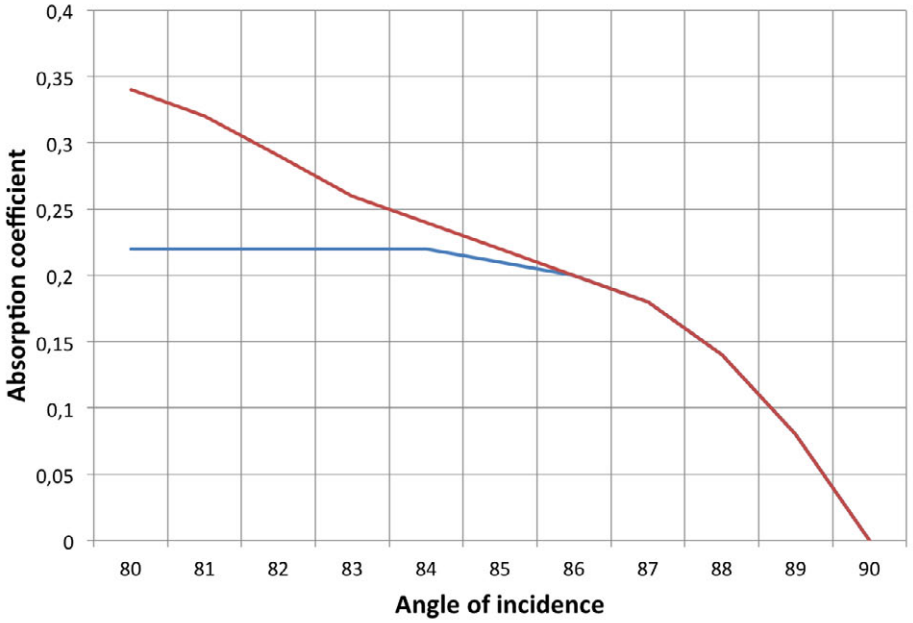

FIGURE 4.14: Absorption coefficient for large angles of incidence. 15 mm material backed by an air cavity of 165 mm (blue) and 785 mm (red)

of the air cavity when local and extended reactions are assumed are also analyzed. Figure 4.15 shows the reverberation times measured and simulated, assuming both local and extended reaction, for configurations 15A and 15B respectively. Discrepancies between simulations and measured values are considerable for both

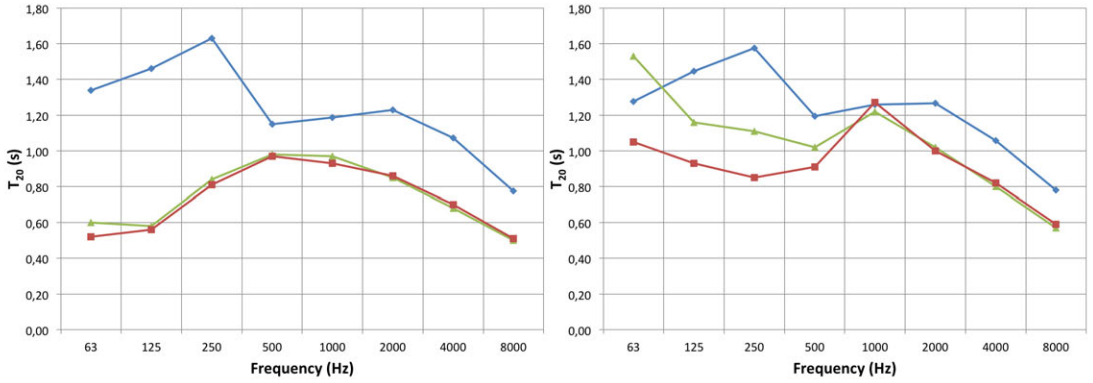

FIGURE 4.15: Values of reverberation time measured (blue) and simulated assuming extended (green) and local (red) reactions for configurations 15A (left) and 15B (right)

thicknesses of air cavity, although the thicker one shows the higher difference. This will be discussed further below. This same tendency is observed for all combinations of materials and configurations. The extended reaction appears to give better results in both cases, although the improvements achieved with respect to the local reaction assumption in cases with thinner air cavities are the higher of

the two. Be that as it may, valid conclusions can not be drawn, owing to the poor simulation results.

Regarding the relationships between the other acoustic parameters measured and the thickness of the air cavity, no relevant conclusions are drawn. For STI, a wide cavity always produces very small improvements in relation to the configurations with thinner air cavities. For this parameter, the introduction of furniture is more relevant, since it produces greater improvements. The values of C_{50} also tend to be higher when the air cavity is thicker. The same pattern is followed for all configurations and materials. However, the values of Sound Strength do not seem to follow any pattern. This makes it impossible to establish relationships with the thickness of the cavity, since the results are different for each frequency band and configuration. Figure 4.16 shows the values of G and C_{50} for configurations 20A and 20B, respectively.

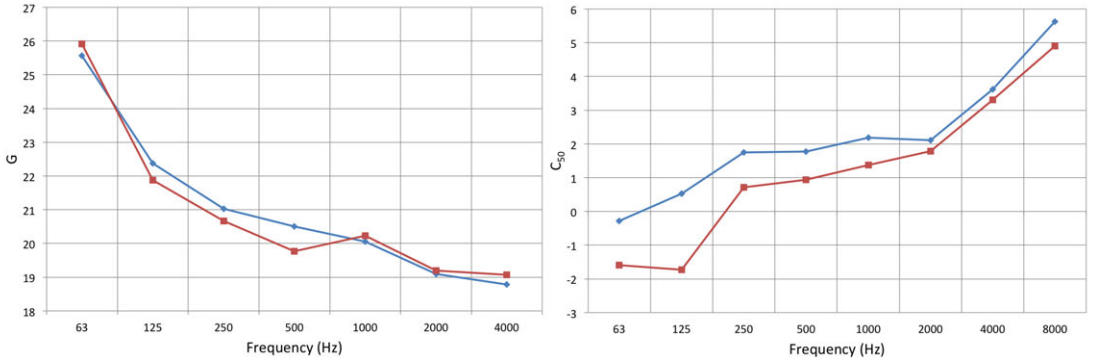

FIGURE 4.16: G (left) and C_{50} (right) measured values for configurations 20A (blue) and 20B (red)

4.4 Simulations

The results of the simulations in terms of reverberation time are compared in this Section with the measured values. In general, the results are not as good as expected throughout the frequency range studied. Large discrepancies between measured and simulated values for almost all configurations are found. Since the simulations seem to have a better correlation with the measured values when extended reaction is assumed, this assumption will be chosen from now on. Figure 4.17 shows the values of reverberation time measured and simulated for configuration 20A. The differences at low frequencies are as expected, owing to the modal behaviour of the room below the cut-off Schroeder frequency, which is not taken

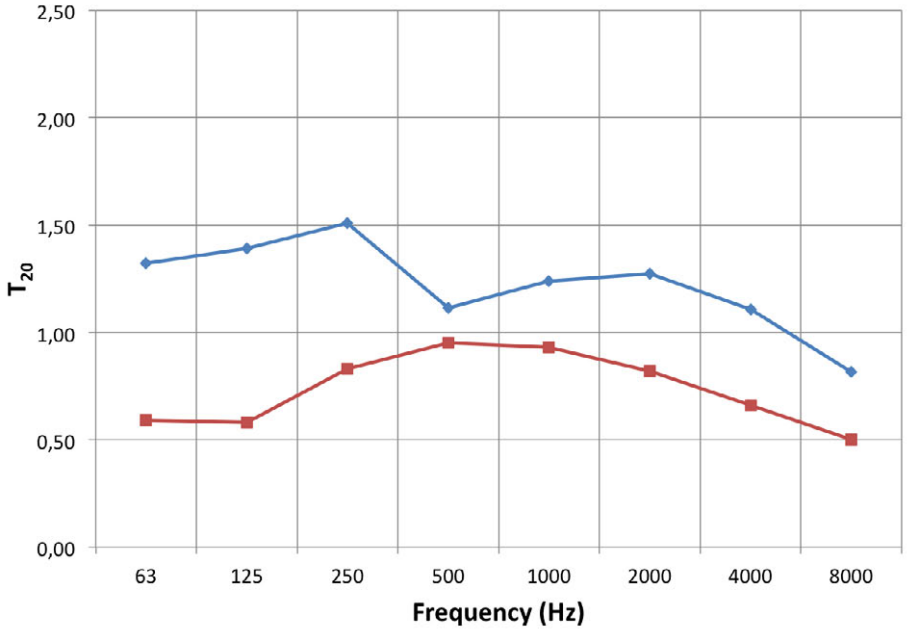

FIGURE 4.17: Configuration 20A. Simulated versus measured T_{20}. Simulations in red, measurements in blue

into account by ODEON. However, the results should be better at high frequencies, where differences involving several JNDs are found. For all materials, the pattern is the same. Reverberation times are underestimated when an overestimation would be normal because of the edge effect, which is not taken into account by ODEON. The explanation for this is again linked to the angle-dependent behaviour of the materials and the division of the sound field into two subfields. Figure 4.18 shows the reverberation times measured and simulated for configurations 20A and 20B. It can be seen that the results are improved when the air cavity

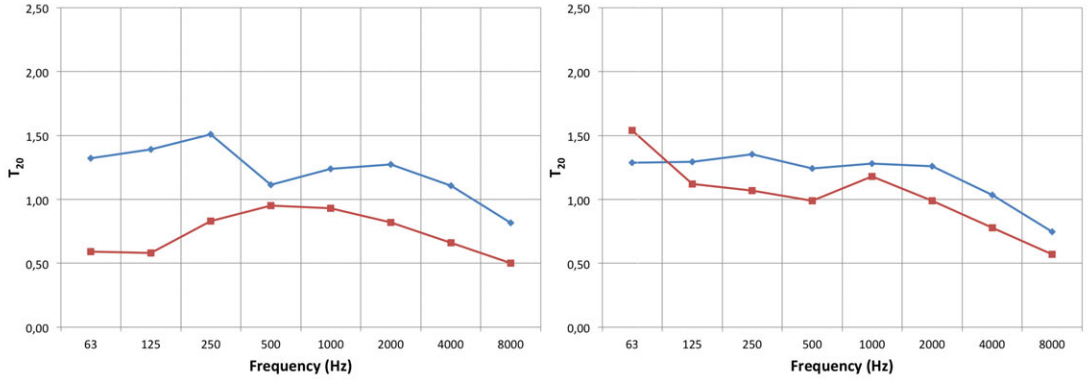

FIGURE 4.18: Simulated versus measured T_{20}. Simulations in red, measurements in blue. Configurations 20A (left) and 20B (right)

backing the suspended ceiling is thinner and hence the dimensions of the room are

larger and more regular. This shape of room generates more diffuse sound fields. For this reason, ODEON simulations, in which the surfaces are characterized by their random incidence absorption coefficients, produce better results. The best results are achieved in configurations involving the thinnest air cavity and furniture, as shown in Figure 4.19, which shows reverberation times measured and simulated for configurations 50B and 50BF. The simulated values for configura-

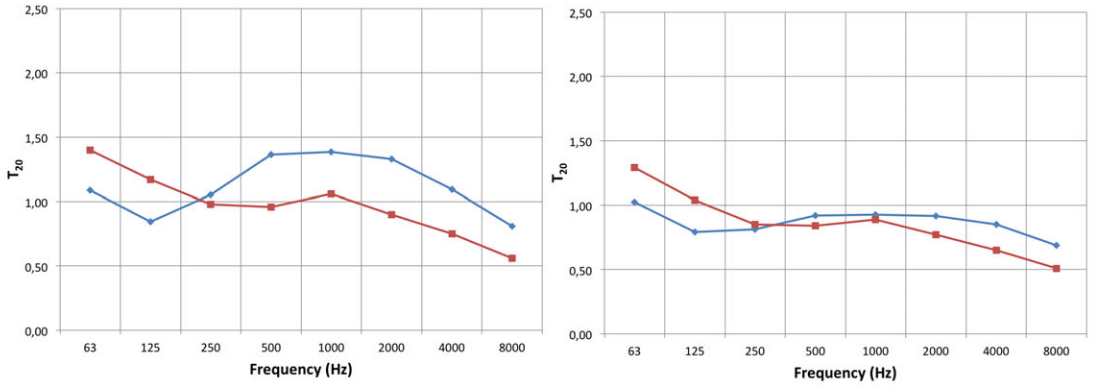

FIGURE 4.19: Simulated versus measured T_{20}. Simulations in red, measurements in blue. Configurations 50B (left) and 50BF (right)

tion 50BF, including furniture, are very similar to those measured, improving the results obtained for the situation with no desks and chairs. This reinforces the theory explained above, since in this case the scattering produces a more diffuse sound field. This means that the random incidence absorption coefficient is a valid descriptor for characterizing the surfaces in these cases.

Note that the angular absorption option has been activated in ODEON for all surfaces in all simulations. If it had not been enabled, the discrepancies would be much larger, as shown in Figure 4.20, which compares the measured reverberation times with those simulated with the angular absorption option, both activated and disabled for configuration 20A.

It is clear from the figure that the angular absorption option improves the simulation results, especially at high frequencies, where the reverberation times are longer when the option is enabled. This indicates that the method reduces absorption at these frequencies in comparison to the value given by the random incidence absorption coefficient. Since the angle-dependent behaviour of each absorber is different, it is reasonable that the angular absorption method can not predict the exact behaviour of the different materials. It is simply a rough approximation, which actually improves the results.

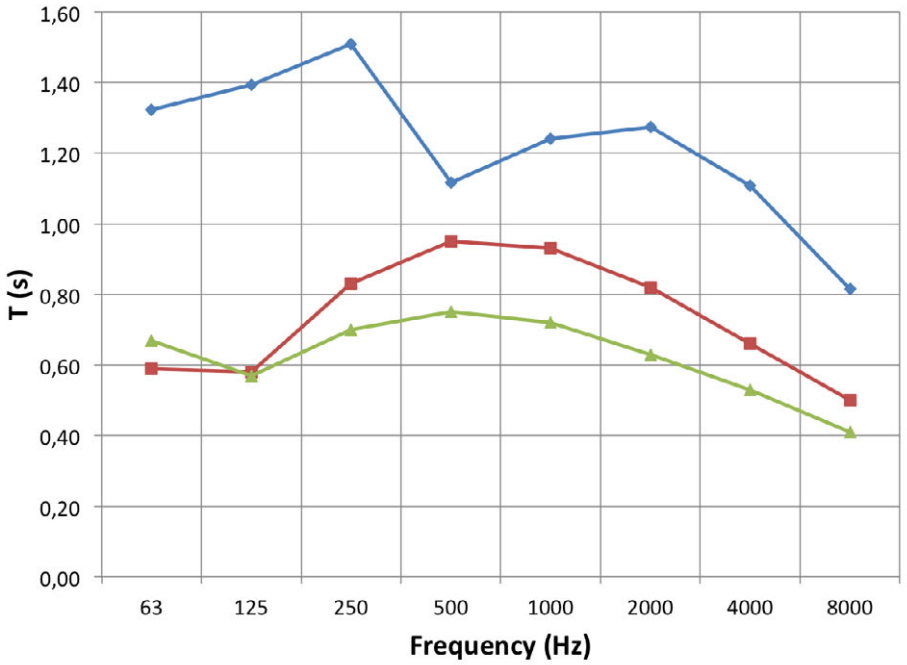

FIGURE 4.20: Values of T_{20} measured (blue), simulated with angular absorption option activated (red) and deactivated (green) for configuration 20A

This fits perfectly with the theory presented in [1], which refers to the tendency of sound waves to hit the absorber from large angles of incidence with respect to the perpendicular direction to the absorber in rooms where one of the surfaces is much more absorbent than the others. The materials used during the completion of this work have lower absorption coefficients at these angles, while, at the same time, the simulations overestimate the absorption. Therefore, if the predominant incidence angles are small and the absorption coefficients at these angles are much lower than those given by the random incidence absorption coefficient, it makes sense that the simulation results always underestimate the reverberation times. The reason is that ODEON does not predict the angle-dependent behaviour of the absorbers accurately.

The range of predominant incidence angles may be approximately estimated by observing the absorption coefficients as a function of incidence angle of the three materials. Figure 4.21 shows the absorption coefficient versus the angle of incidence of the three materials at a frequency of 1000 Hz.

At this frequency, the random incidence absorption coefficients of the materials of 15, 20, and 50 mm are, respectively, 0,71, 0,75 and 0,85. In a room with a diffuse sound field, the reverberation time at 1000 Hz should be longer when the

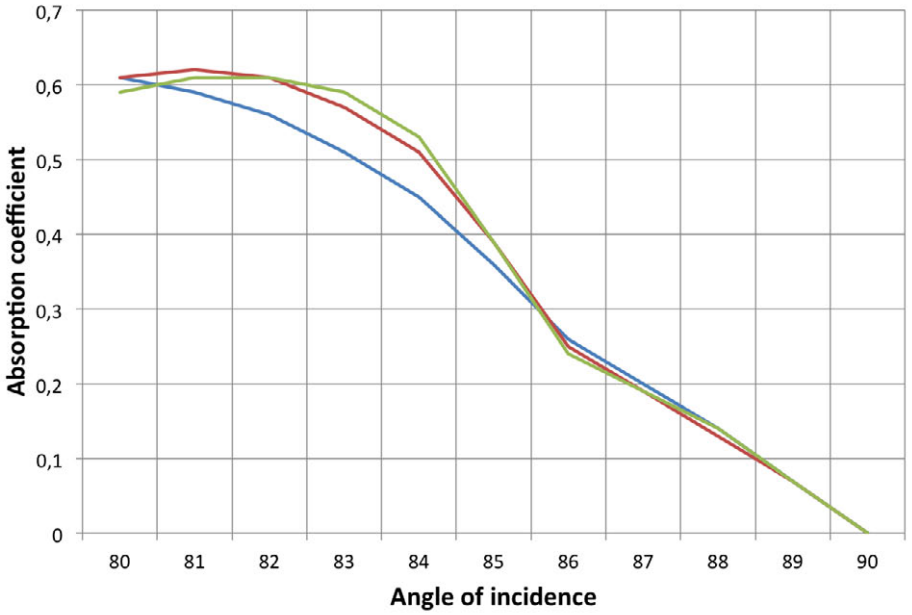

FIGURE 4.21: Absorption coefficient at 1000 Hz as a function of incidence angle. 50 mm (blue), 20 mm (red) and 15 mm (green)

material of 15 mm is placed due to its lower absorption compared to the other two materials. However, the measured reverberation times show the opposite. They are 1.19 s for 15 mm, 1.24 s for 20 mm and 1.36 for the material of 50 mm. It can be deduced from Figure 4.21, that the predominant angles of incidence at this frequency must be between 81 and 86 degrees with respect to the direction perpendicular to the absorber, in other words, between 4 and 9 degrees respect to the absorbent. Within this angle range, the absorption follows a completely opposite pattern to the values of random incidence absorption coefficient. This value is greater when the material is thinner. This explains why, throughout this entire work, lower values of random incidence absorption coefficient have produced shorter reverberation times than those obtained with larger absorption coefficients and vice versa.

CHAPTER 5

Conclussion

5.1 Summary

Impulse Response measurements according to ISO 3382 are carried out in the laboratories of the company Ecophon in Hyllinge, creating different acoustic scenarios which simulate those found in a classroom. Different porous materials are placed as wall panels and ceilings and their height is varied in order to create the greatest number of possible conditions. In addition, pieces of furniture such as desks and chairs are introduced into the room. From the Impulse Responses, several acoustical parameters such as T_{20}, EDT, C_{50}, G and STI are obtained and compared to see the effect produced on them when the combinations of the above materials are varied. Furthermore, in order to characterize the materials in the most accurate possible way, their impedances are measured in a Kundt's tube at DTU.

All configurations recreated in Hyllinge, are simulated using ODEON. As a descriptor for the surfaces, the random incidence absorption coefficient is used. This is obtained by Miki's Model, assuming both local and extended reactions. The simulated reverberation times are compared with the measurements and conclusions are drawn about the performance of the different methods.

From the values of the acoustical parameters obtained by the measurements, it is observed that the absorption is not enough in all configurations to meet the requirements established by the Danish regulations regarding reverberation time, especially at low frequencies. It is essential to achieve low reverberation times at these frequencies in order to reduce masking effect on speech. Therefore, more

effort should be dedicated to improve absorption within this range. Nevertheless, STI values are good in all configurations including absorbers.

Moreover, shorter reverberation times are achieved with materials having lower random incidence absorption coefficients . Furthermore, in contrast to what is expected, when suspended ceilings are backed by thicker air cavities, their absorptions are lower at low frequencies.

In rooms including a surface which is much more absorptive than the others, the sound field is far from diffuse. Under these conditions, a division of the sound field into two subfields, grazing and non-grazing, occurs. This renders Sabine's formula invalid for the prediction of the behaviour of the sound field and for finding different values of reverberation time depending on the section of the decay curve chosen. Moreover, in the above-mentioned rooms, sound waves tend to hit the highly absorptive surface from small angles of incidence with respect to the material. Generally, the absorption of porous absorbers for these angles is lower than for the rest. Both the introduction of furniture, which increases the scattering, and the placement of the ceiling as high as possible, thereby changing the shape of the room to a more regular form, increase the diffusion. This causes the sound waves to hit the absorber from a wider range of angles and therefore increases the absorption.

The ODEON simulation results are worse than expected. Significant discrepancies are found between measured and simulated values throughout the entire frequency range. Below the cut-off Schroeder frequency, the results are not reliable, since ODEON ignores the modal behaviour of the room. The diffraction effect is not taken into account by ODEON. This causes discrepancies in all frequency bands for configurations including wall panels, where reverberation times are overestimated. At high frequencies, where an overestimation of reverberation times owing to diffraction is expected, the result is the opposite. This is also explained by the angle-dependent behaviour of the materials, which is not modeled correctly by ODEON, even when the angular absorption option is enabled.

Regarding the local and extended reaction assumptions, although a definitive conclusion can not be drawn, the latter seems to better model the behaviour of the materials when backed by an air cavity.

5.2 Future work

Noting the weaknesses of ODEON, particularly in relation to the angle-dependent behaviour of the materials, the development of the PARISM model seems essential if an accurate simulation tool is to be found that does not increase excessively the computational time for this kind of room.

An extension of this work, with a greater focus on the other measured acoustical parameters, would be very interesting, owing to the emerging trend that does not consider reverberation time as the only descriptor of the acoustic quality of a room.

A comparative study between the measured values and those obtained with different empirical formulas could also be an interesting addition to this work. The objective would be to find a formula that better adjusts to the behaviour of these rooms.

Although a large number of measurements were made for the configuration 20AF (most typical classroom) in order to study the repeatability in such rooms, that study has not been included in this paper due to lack of time.

Appendix A

Measurements

Frequency (Hz)	**63**	**125**	**250**	**500**	**1000**	**2000**	**4000**	**8000**
EDT (s)	1.12	1.28	1.37	1.04	1.12	1.10	0.84	0.65
$\mathbf{T_{20}}$ (s)	1.32	1.39	1.50	1.11	1.24	1.27	1.10	0.81
$\mathbf{C_{50}}$ (dB)	-0.29	0.53	1.75	1.77	2.18	2.11	3.62	5.62
G (dB)	25.57	22.37	21.03	20.50	20.05	19.1	18.78	-230.76
STI	0.64							

Table A.1: Configuration 20A. 20 mm ceiling, 780 mm air gap, no furniture, no wall absorbers

Frequency (Hz)	**63**	**125**	**250**	**500**	**1000**	**2000**	**4000**	**8000**
EDT (s)	1.08	1.30	1.30	0.73	0.70	0.78	0.69	0.59
$\mathbf{T_{20}}$ (s)	1.28	1.39	1.42	0.80	0.77	0.90	0.89	0.70
$\mathbf{C_{50}}$ (dB)	-0.31	-0.39	1.53	3.68	4.10	3.73	4.49	5.95
G (dB)	25.55	21.85	20.58	19.56	18.82	18.15	17.69	-231.73
STI	0.68							

Table A.2: Configuration 20AF. 20 mm ceiling, 780 mm air gap, furniture, no wall absorbers

Frequency (Hz)	**63**	**125**	**250**	**500**	**1000**	**2000**	**4000**	**8000**
EDT (s)	0.91	1.31	1.33	0.71	0.66	0.67	0.51	0.45
$\mathbf{T_{20}}$ (s)	1.28	1.41	1.42	0.82	0.72	0.83	0.76	0.58
$\mathbf{C_{50}}$ (dB)	0.92	-0.23	0.67	3.47	4.56	5.23	5.59	6.78
G (dB)	26.5	22.33	20.23	18.91	17.70	18.04	17.55	-231.72
STI	0.71							

Table A.3: Configuration 20AFe. 20 mm ceiling, 780 mm air gap, furniture, no wall absorbers. Extra source and microphone heights

Frequency (Hz)	**63**	**125**	**250**	**500**	**1000**	**2000**	**4000**	**8000**
EDT (s)	1.11	1.30	1.37	1.00	1.01	1.01	0.81	0.59
$\mathbf{T_{20}}$ (s)	1.31	1.38	1.49	1.06	1.12	1.16	1.03	0.78
$\mathbf{C_{50}}$ (dB)	-0.28	0.18	1.25	1.78	2.31	2.74	4.12	6.04
G (dB)	25.56	22.24	20.81	20.52	19.76	19.06	18.69	-230.51
STI	0.65							

Table A.4: Configuration 20Af. 20 mm ceiling, 780 mm air gap, furniture, no wall absorbers. Only 1 set of desk and 2 chairs

Frequency (Hz)	**63**	**125**	**250**	**500**	**1000**	**2000**	**4000**	**8000**
EDT (s)	1.13	1.35	1.48	1.06	1.06	1.02	0.78	0.57
$\mathbf{T_{20}}$ (s)	1.33	1.46	1.63	1.15	1.18	1.22	1.07	0.77
$\mathbf{C_{50}}$ (dB)	-0.55	-0.25	0.71	0.99	2.13	2.91	4.28	5.68
G (dB)	25.68	22.43	21.32	20.97	20.23	19.46	18.97	-230.74
STI	0.64							

Table A.5: Configuration 15A. 15 mm ceiling, 785 mm air gap, no furniture, no wall absorbers

Frequency (Hz)	**63**	**125**	**250**	**500**	**1000**	**2000**	**4000**	**8000**
EDT (s)	1.11	1.35	1.40	0.79	0.68	0.74	0.65	0.50
$\mathbf{T_{20}}$ (s)	1.30	1.44	1.51	0.86	0.76	0.88	0.84	0.65
$\mathbf{C_{50}}$ (dB)	-0.65	-1.35	0.65	2.75	4.49	3.93	4.95	6.51
G (dB)	25.64	22.01	20.82	19.84	19.34	18.44	17.93	-231.38
STI	0.69							

Table A.6: Configuration 15AF. 15 mm ceiling, 785 mm air gap, furniture, no wall absorbers

Frequency (Hz)	**63**	**125**	**250**	**500**	**1000**	**2000**	**4000**	**8000**
EDT (s)	1.00	0.98	0.75	1.06	1.24	1.16	0.93	0.67
$\mathbf{T_{20}}$ (s)	1.19	1.03	0.94	1.19	1.36	1.33	1.09	0.79
$\mathbf{C_{50}}$ (dB)	0.04	2.44	4.33	1.44	1.41	1.36	3.12	5.13
G (dB)	24.67	19.74	19.23	19.93	20.16	19.40	18.58	-231.39
STI	0.63							

Table A.7: Configuration 50A. 50 mm ceiling, 750 mm air gap, no furniture, no wall absorbers

Frequency (Hz)	**63**	**125**	**250**	**500**	**1000**	**2000**	**4000**	**8000**
EDT (s)	0.97	1.02	0.67	0.72	0.78	0.87	0.75	0.62
$\mathbf{T_{20}}$ (s)	1.13	1.03	0.81	0.75	0.82	0.92	0.87	0.71
$\mathbf{C_{50}}$ (dB)	-0.10	1.35	4.83	3.77	3.22	3.12	4.01	5.46
G (dB)	24.68	19.25	18.95	18.85	18.82	18.43	17.64	-232.44
STI	0.68							

Table A.8: Configuration 50AF. 50 mm ceiling, 750 mm air gap, furniture, no wall absorbers

Frequency (Hz)	**63**	**125**	**250**	**500**	**1000**	**2000**	**4000**	**8000**
EDT (s)	1.06	1.24	1.20	0.79	0.70	0.65	0.57	0.47
$\mathbf{T_{20}}$ (s)	1.24	1.32	1.32	0.84	0.81	0.79	0.76	0.63
$\mathbf{C_{50}}$ (dB)	-0.11	0.59	2.34	3.80	4.59	4.63	5.94	7.39
G (dB)	25.37	22.14	20.34	19.77	18.75	17.81	17.71	-231.14
STI	0.71							

Table A.9: Configuration 20AW. 20 mm ceiling, 780 mm air gap, no furniture, wall absorbers

Frequency (Hz)	**63**	**125**	**250**	**500**	**1000**	**2000**	**4000**	**8000**
EDT (s)	1.04	1.25	1.16	0.62	0.49	0.56	0.48	0.41
$\mathbf{T_{20}}$ (s)	1.21	1.32	1.23	0.67	0.60	0.65	0.68	0.57
$\mathbf{C_{50}}$ (dB)	-0.23	-0.65	2.00	4.78	6.21	5.50	6.62	8.08
G (dB)	25.36	21.77	19.92	19.2	18.19	17.07	17.3	-231.63
STI	0.74							

Table A.10: Configuration 20AFW. 20 mm ceiling, 780 mm air gap, furniture, wall absorbers

Frequency (Hz)	**63**	**125**	**250**	**500**	**1000**	**2000**	**4000**	**8000**
EDT (s)	1.08	1.26	1.23	1.12	1.13	1.08	0.80	0.60
$\mathbf{T_{20}}$ (s)	1.28	1.29	1.35	1.24	1.27	1.26	1.03	0.74
$\mathbf{C_{50}}$ (dB)	-1.59	-1.73	0.71	0.94	1.37	1.78	3.31	4.90
G (dB)	25.91	21.88	20.66	19.77	20.23	19.19	19.07	-231.17
STI	0.62							

Table A.11: Configuration 20B. 20 mm ceiling, 160 mm air gap, no furniture, no wall absorbers

Frequency (Hz)	**63**	**125**	**250**	**500**	**1000**	**2000**	**4000**	**8000**
EDT (s)	1.04	1.20	1.13	0.81	0.73	0.81	0.64	0.50
$\mathbf{T_{20}}$ (s)	1.22	1.24	1.28	0.81	0.86	0.86	0.81	0.64
$\mathbf{C_{50}}$ (dB)	-1.52	-2.10	0.98	2.99	3.62	3.08	4.53	6.21
G (dB)	26.11	22.56	20.78	18.53	19.23	18.13	18.20	-231.60
STI	0.68							

Table A.12: Configuration 20BF. 20 mm ceiling, 160 mm air gap, furniture, no wall absorbers

Frequency (Hz)	**63**	**125**	**250**	**500**	**1000**	**2000**	**4000**	**8000**
EDT (s)	1.08	1.30	1.41	1.08	1.09	1.05	0.84	0.65
$\mathbf{T_{20}}$ (s)	1.27	1.44	1.57	1.19	1.25	1.26	1.05	0.78
$\mathbf{C_{50}}$ (dB)	-1.46	-2.44	-0.19	1.06	1.16	1.82	3.32	4.39
G (dB)	25.87	22.21	21.33	19.7	20.34	19.54	19.61	-230.46
STI	0.62							

Table A.13: Configuration 15B. 15 mm ceiling, 165 mm air gap, no furniture, no wall absorbers

Frequency (Hz)	**63**	**125**	**250**	**500**	**1000**	**2000**	**4000**	**8000**
EDT (s)	1.03	1.24	1.27	0.80	0.75	0.80	0.66	0.55
$\mathbf{T_{20}}$ (s)	1.22	1.38	1.46	0.81	0.85	0.87	0.83	0.66
$\mathbf{C_{50}}$ (dB)	-1.40	-2.10	0.26	3.08	3.34	3.19	3.96	5.09
G (dB)	26.20	22.90	21.48	18.62	19.3	18.64	18.71	-231.09
STI	0.67							

Table A.14: Configuration 15BF. 15 mm ceiling, 165 mm air gap, furniture, no wall absorbers

Frequency (Hz)	**63**	**125**	**250**	**500**	**1000**	**2000**	**4000**	**8000**
EDT (s)	0.92	0.80	0.80	1.19	1.25	1.18	0.92	0.68
$\mathbf{T_{20}}$ (s)	1.08	0.84	1.05	1.36	1.38	1.32	1.09	0.80
$\mathbf{C_{50}}$ (dB)	-0.71	2.21	2.38	0.47	0.86	1.30	3.03	4.70
G (dB)	24.92	19.94	20.61	20.26	20.23	19.51	19.29	-230.79
STI	0.62							

Table A.15: Configuration 50B. 50 mm ceiling, 130 mm air gap, no furniture, no wall absorbers

Frequency (Hz)	**63**	**125**	**250**	**500**	**1000**	**2000**	**4000**	**8000**
EDT (s)	0.90	0.79	0.70	0.84	0.85	0.88	0.70	0.59
$\mathbf{T_{20}}$ (s)	1.02	0.79	0.81	0.92	0.92	0.91	0.85	0.68
$\mathbf{C_{50}}$ (dB)	-0.96	1.84	3.17	2.27	2.69	2.43	3.70	5.19
G (dB)	25.37	20.63	20.25	19.06	19.09	18.22	18.35	-231.67
STI	0.67							

Table A.16: Configuration 50BF. 50 mm ceiling, 130 mm air gap, furniture, no wall absorbers

Frequency (Hz)	**63**	**125**	**250**	**500**	**1000**	**2000**	**4000**	**8000**
EDT (s)	1.03	1.23	1.05	0.84	0.75	0.69	0.55	0.44
$\mathbf{T_{20}}$ (s)	1.21	1.27	1.22	0.86	0.83	0.80	0.71	0.57
$\mathbf{C_{50}}$ (dB)	-1.35	-1.84	1.49	2.94	3.69	4.26	5.55	7.13
G (dB)	25.71	21.84	20.38	18.56	18.74	18.09	18.27	-231.25
STI	0.70							

Table A.17: Configuration 20BW. 20 mm ceiling, 160 mm air gap, no furniture, wall absorbers

Frequency (Hz)	**63**	**125**	**250**	**500**	**1000**	**2000**	**4000**	**8000**
EDT (s)	1.01	1.18	1.04	0.66	0.56	0.59	0.49	0.42
$\mathbf{T_{20}}$ (s)	1.15	1.19	1.13	0.65	0.63	0.64	0.62	0.51
$\mathbf{C_{50}}$ (dB)	-1.43	-1.79	1.53	4.62	4.93	5.00	5.87	7.40
G (dB)	25.88	22.39	20.44	17.72	18.06	17.12	17.31	-232.20
STI	0.72							

Table A.18: Configuration 20BFW. 20 mm ceiling, 160 mm air gap, furniture, wall absorbers

Frequency (Hz)	**63**	**125**	**250**	**500**	**1000**	**2000**	**4000**	**8000**
EDT (s)	1.34	2.07	3.00	3.83	3.58	2.47	1.64	1.09
$\mathbf{T_{20}}$ (s)	1.60	2.46	3.07	3.87	3.62	2.58	1.70	1.15
$\mathbf{C_{50}}$ (dB)	-2.28	-5.52	-6.43	-7.57	-6.20	-4.73	-2.55	0.23
G (dB)	27.07	25.57	27.5	28.16	27.98	26.38	24.52	-227.34
STI	0.41							

TABLE A.19: Configuration E. No suspended ceiling, no furniture, no wall absorbers

Frequency (Hz)	**63**	**125**	**250**	**500**	**1000**	**2000**	**4000**	**8000**
EDT (s)	1.24	1.92	2.45	2.71	2.20	1.63	1.20	0.87
$\mathbf{T_{20}}$ (s)	1.72	2.27	2.50	2.68	2.26	1.68	1.22	0.88
$\mathbf{C_{50}}$ (dB)	-3.22	-4.65	-5.40	-4.75	-3.84	-2.42	-0.63	1.51
G (dB)	28.19	26.29	26.86	26.51	25.73	24.54	23.13	-228.18
STI	0.48							

TABLE A.20: Configuration F. No suspended ceiling, furniture, no wall absorbers

Frequency (Hz)	**63**	**125**	**250**	**500**	**1000**	**2000**	**4000**	**8000**
EDT (s)	1.25	1.92	2.15	1.91	1.75	1.49	1.23	0.96
$\mathbf{T_{20}}$ (s)	1.48	2.19	2.15	1.95	1.79	1.56	1.28	0.96
$\mathbf{C_{50}}$ (dB)	-1.94	-4.97	-4.76	-3.54	-2.32	-2.06	-0.78	1.02
G (dB)	26.82	25.13	26.07	25.07	24.90	24.24	23.32	-227.84
STI	0.50							

TABLE A.21: Configuration W. No suspended ceiling, no furniture, wall absorbers

Frequency (Hz)	**63**	**125**	**250**	**500**	**1000**	**2000**	**4000**	**8000**
EDT (s)	1.18	1.79	1.88	1.60	1.32	1.14	0.96	0.78
$\mathbf{T_{20}}$ (s)	1.57	2.08	1.94	1.63	1.36	1.16	0.98	0.78
$\mathbf{C_{50}}$ (dB)	-2.83	-4.07	-4.46	-2.54	-0.91	-0.46	0.53	2.32
G (dB)	27.68	25.75	25.65	24.41	23.84	23.11	22.30	-228.34
STI	0.55							

TABLE A.22: Configuration FW. No suspended ceiling, furniture, wall absorbers

Appendix B

Complete results of simulations

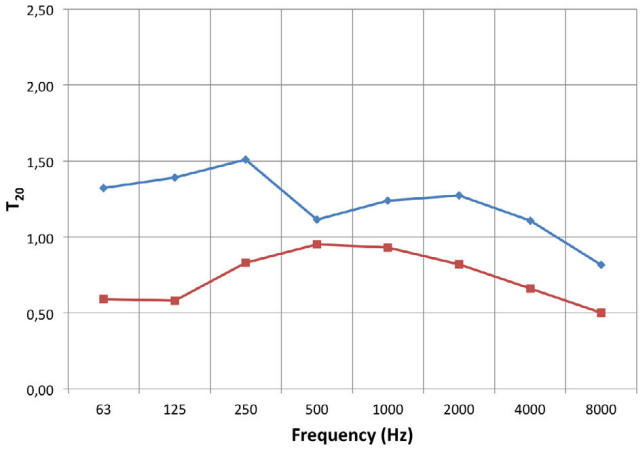

FIGURE B.1: Configuration 20A. Simulated versus measured T_{20}. Simulations in red, measurements in blue

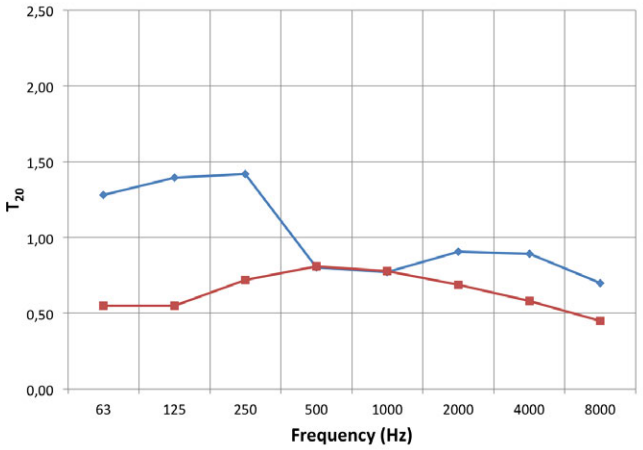

FIGURE B.2: Configuration 20AF. Simulated versus measured T_{20}. Simulations in red, measurements in blue

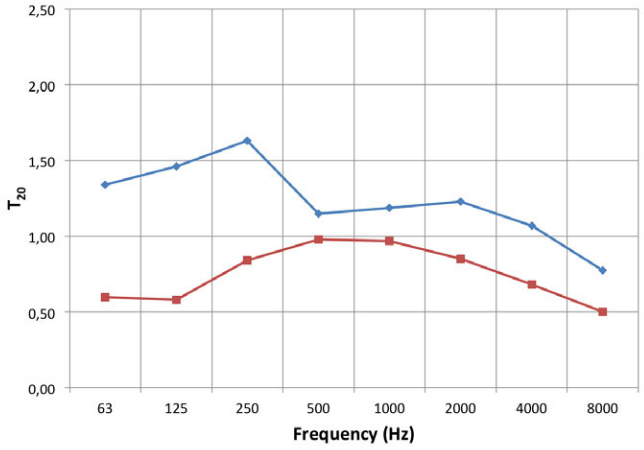

FIGURE B.3: Configuration 15A. Simulated versus measured T_{20}. Simulations in red, measurements in blue

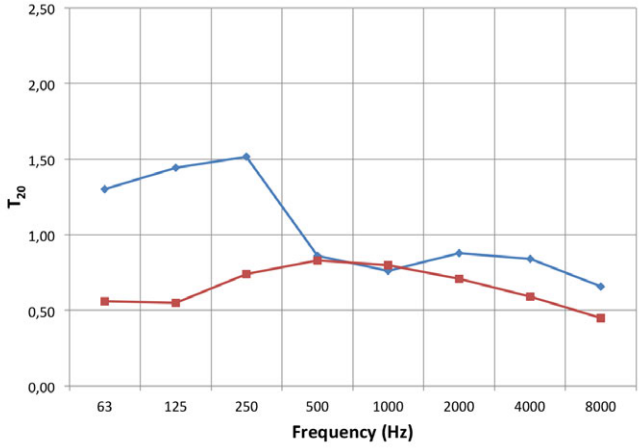

FIGURE B.4: Configuration 15AF. Simulated versus measured T_{20}. Simulations in red, measurements in blue

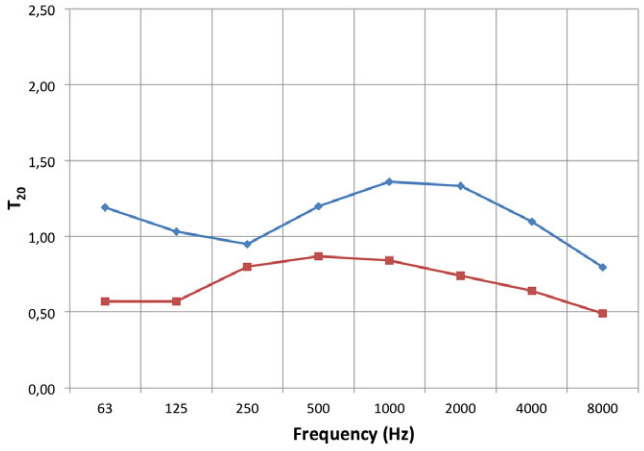

FIGURE B.5: Configuration 50A. Simulated versus measured T_{20}. Simulations in red, measurements in blue

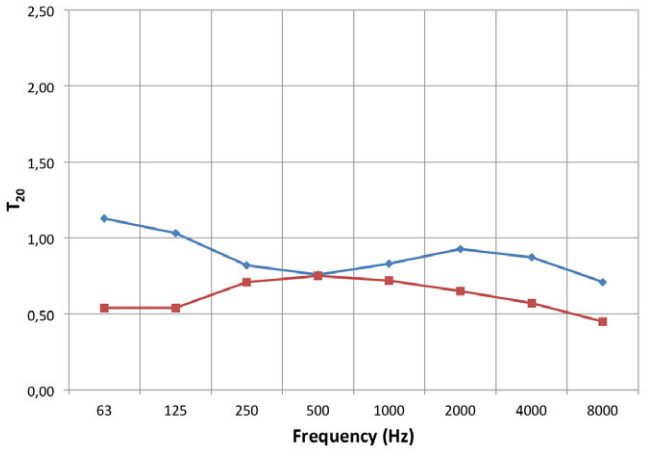

FIGURE B.6: Configuration 50AF. Simulated versus measured T_{20}. Simulations in red, measurements in blue

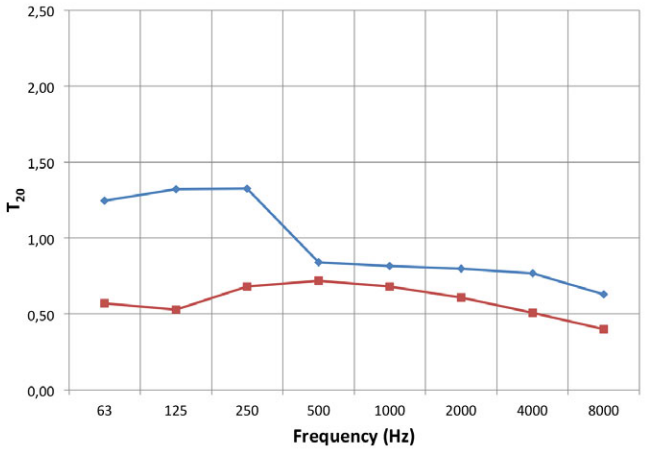

FIGURE B.7: Configuration 20AW. Simulated versus measured T_{20}. Simulations in red, measurements in blue

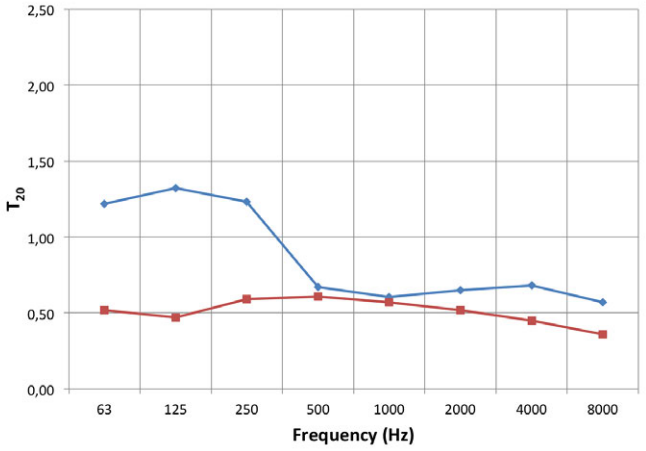

FIGURE B.8: Configuration 20AFW. Simulated versus measured T_{20}. Simulations in red, measurements in blue

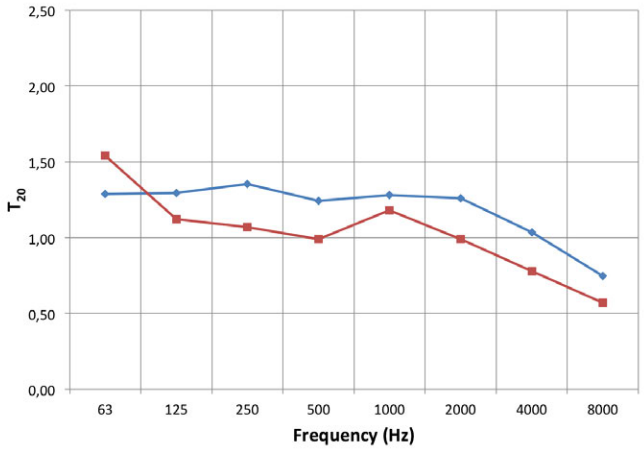

FIGURE B.9: Configuration 20B. Simulated versus measured T_{20}. Simulations in red, measurements in blue

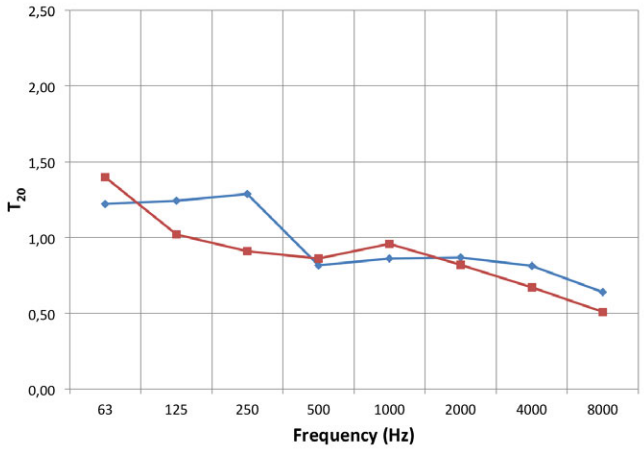

FIGURE B.10: Configuration 20BF. Simulated versus measured T_{20}. Simulations in red, measurements in blue

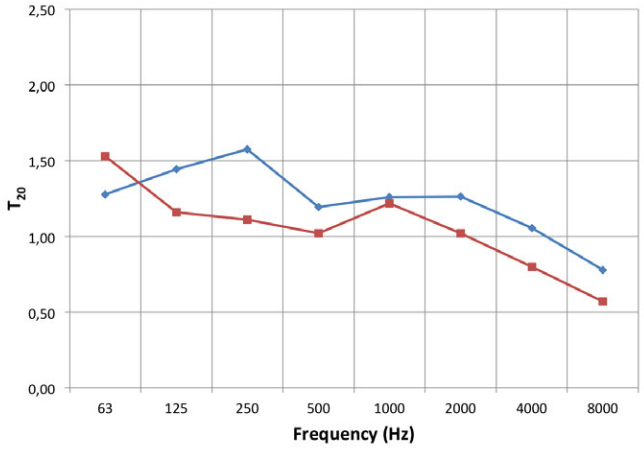

FIGURE B.11: Configuration 15B. Simulated versus measured T_{20}. Simulations in red, measurements in blue

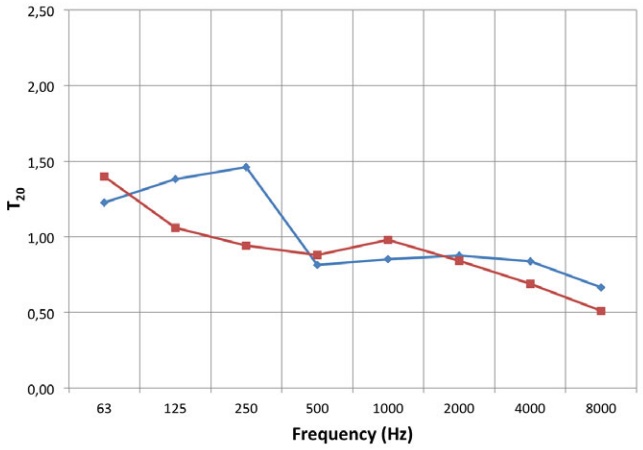

FIGURE B.12: Configuration 15BF. Simulated versus measured T_{20}. Simulations in red, measurements in blue

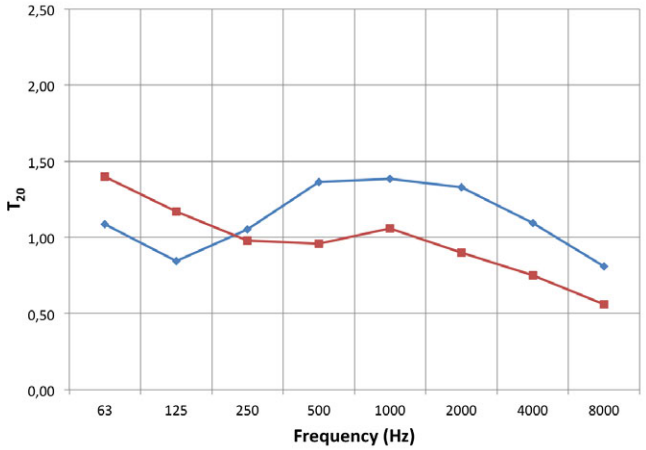

FIGURE B.13: Configuration 50B. Simulated versus measured T_{20}. Simulations in red, measurements in blue

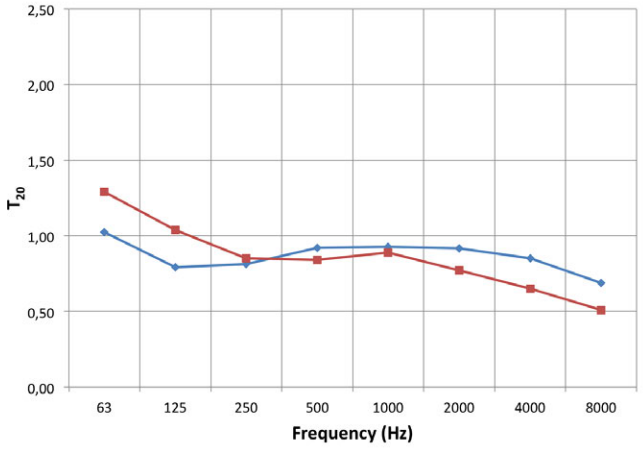

FIGURE B.14: Configuration 50BF. Simulated versus measured T_{20}. Simulations in red, measurements in blue

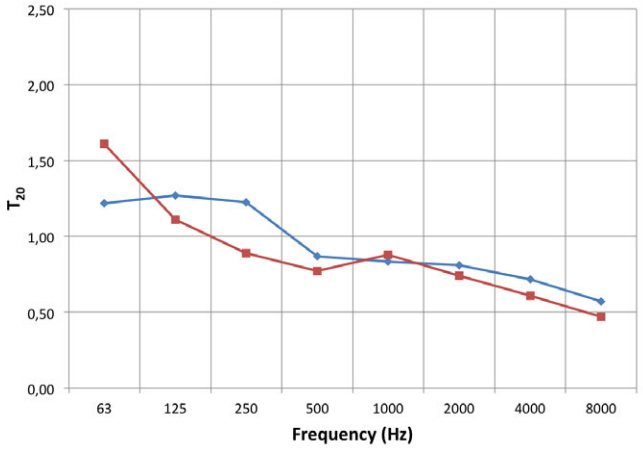

FIGURE B.15: Configuration 20BW. Simulated versus measured T_{20}. Simulations in red, measurements in blue

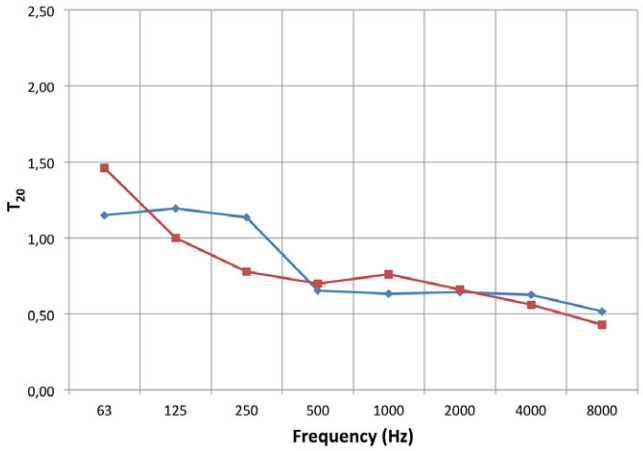

FIGURE B.16: Configuration 20BFW. Simulated versus measured T_{20}. Simulations in red, measurements in blue

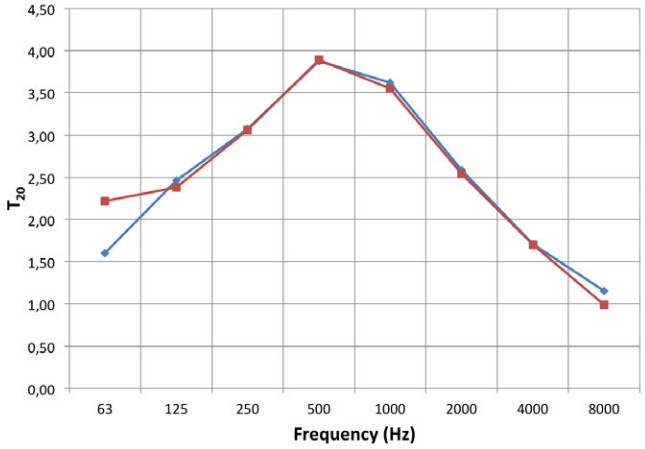

FIGURE B.17: Configuration E. Simulated versus measured T_{20}. Simulations in red, measurements in blue

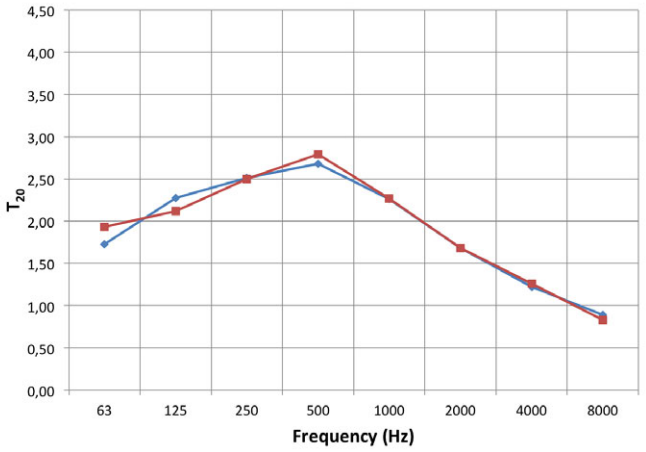

FIGURE B.18: Configuration F. Simulated versus measured T_{20}. Simulations in red, measurements in blue

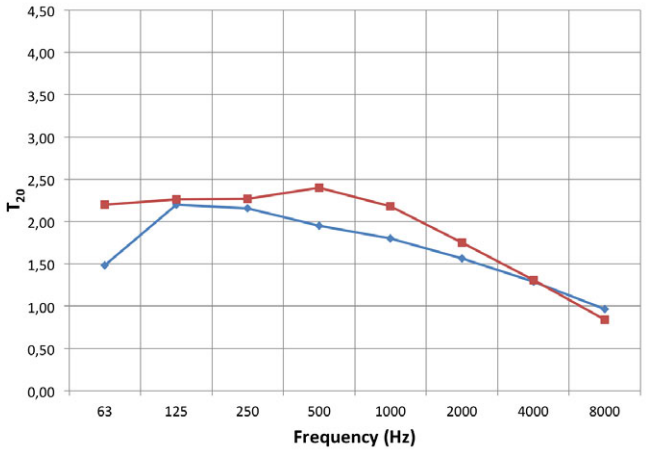

FIGURE B.19: Configuration W. Simulated versus measured T_{20}. Simulations in red, measurements in blue

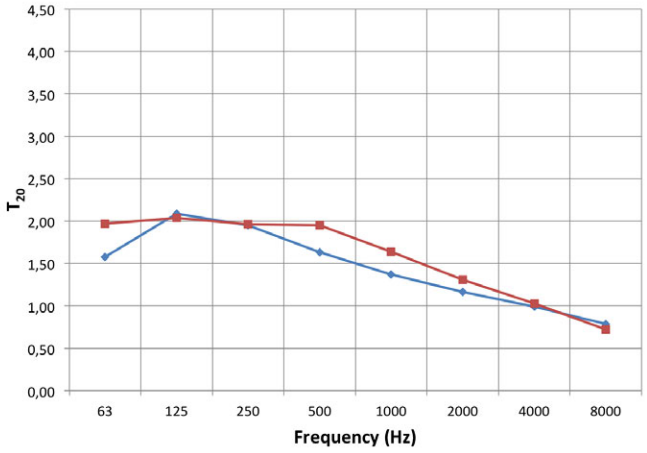

FIGURE B.20: Configuration FW. Simulated versus measured T_{20}. Simulations in red, measurements in blue

List of Figures

List of Tables

Bibliography

1. Marbjerg GH., Brunskog J., Jeong C-H., Nilsson E. “Development of a pressure based room acoustic model using impedance descriptions of surfaces”. Proceedings of Internoise 2013. (2013)

2. Spändock F. “Akustische Modellversuche”. Annalen der Physik. Vol. 412, no 4. (1934)

3. Meyer E. “Reverberation and Absorption of Sound”. Journal of the Acoustical Society of America. Vol 8, Issue 3. (1937)

4. Spencer G.H., Murty M. V. R.K. ”General ray tracing Procedure”. Journal of the Optical Society of America. Vol. 52, Issue 6. (1962)

5. Kulowski.A. “Algorithmic Representation of the Ray Tracing Technique”. Applied Acoustics 18. (1985)

6. Dadoun N., Kirkpatrick D.G., Walsh J.P. “The Geometry of Beam Tracing”. Association for Computer Machinery. (1985)

7. Wayman J.L., Vanyo J.P. ”Three-dimensional computer simulation of reverberation in an enclosure”. Journal of the Acoustical Society of America. Vol. 62, no 1. (1977)

8. Kuttruff H. “Room Acoustics”. 4 ed. London: Spon Press. (2000)

9. Lewers. T. “A Combined Beam Tracing and Radiant Exchange Computer Model of Room Acoustics”. Applied Acoustics 38. (1993)

10. Allen J.B., Berkley D.A. “Image method for efficiently simulating small-room acoustics”. Journal of the Acoustical Society of America, Vol. 65, no 4. (1979)

11. Vorländer M. "Simulation of the transient and steady-state sound propagation in rooms using a new combined ray-tracing / image-source algorithm". Journal of the Acoustical Society of America. Vol. 86, no 1. (1989)

12. Kleiner M.,Dalenbäck B-I., Svensson P. "Auralization-An Overview" Journal Audio Engineering Society. Vol 41, no 11 (1993)

13. Valeai V., Sakout A., Li F. "Solving the diffusion equation with a finite element solver: Calculation of diffuse sound field in room acoustic". Pan-American/Iberian Meeting on Acoustics. Journal of the Acoustical Society of America. Vol. 112, no 5. (2002)

14. Hunter P., Pullan A. "FEM/BEM notes". The University of Auckland, New Zealand. (2001)

15. Yousefzadeh B., Hodgson M. "Energy- and wave-based beam-tracing prediction of room-acoustical parameters using different boundary conditions". Journal of the Acoustical Society of America. Vol. 132, no 3. (2012)

16. Vigran T.E. "Building Acoustics". Chapter 7. Taylor and Francis. (2008)

17. Wareing A., Hodgson M. "Beam-tracing model for predicting sound fields in rooms with multilayer bounding surfaces". The Journal of the Acoustical Society of America. Vol. 118. (2005)

18. Klatte M., Hellbrück J. "Effects of classroom acoustics on performance and well-being in elementary school children: A field study". Proceedings of Internoise 2010. (2010)

19. Shield B.M., Dockrell J.E. "The effects of noise on children at school: a review". Journal of Building Acoustics. Vol. 10, no 2. (2003)

20. Long. M. "Architectural Acoustics" Chapter 17. Elsevier Academic Press. (2006)

21. Carrión A. "Diseño acústico de espacios arquitectónicos". Chapter 3. Edicions UPC. (1998)

22. ISO 3382 – 1: 2009. "Acoustics – Measurement of room acoustic parameters – Part 1: Performance spaces". (2009)

23. ISO 3382 – 2: 2008. Acoustics – Measurement of room acoustic parameters – Part 2 : Reverberation time in ordinary rooms". (2008)

24. IEC 60268. "Sound system equipment – Part 16: Objective rating of speech intelligibility by speech transmission index". (2003)

25. Hak C. C. J. M., Wenmaekers R. H. C., van Luxemburg L. C. J. "Measuring Room Impulse Responses: Impact of the Decay Range on Derived Room Acoustic Parameters". Acta Acustica united with Acustica. Vol. 98, no 6. (2012)

26. Rasmussen B., Brunskog J., Hoffmeyer D. "Reverberation time in class rooms – Comparison of regulation and classification criteria in the Nordic countries". Proceedings of Baltic-Nordic Acoustics Meeting 2012. (2012)

27. Soulodre G.A., Bradley J.S. "Subjective evaluation of new room acoustic measures". The Journal of the Acoustical Society of America. Vol. 98. (1995)

28. Nilsson E. "Room acoustic measures for classrooms" Proceedings of Internoise 2010. (2010)

29. Bistafa S.R., Bradley J.S. "Predicting reverberation times in a simulated classroom". The Journal of the Acoustical Society of America. Vol. 108, no. 4. (2000)

30. Bradley J.S. "Review of objective room acoustics measures and future needs". Proceedings of the International Symposium on Room Acoustics 2010. (2010)

31. Bistafa S.R., Bradley J.S. "Predicting speech metrics in a simulated classroom with varied sound absorption". The Journal of the Acoustical Society of America. Vol. 109, no. 4. (2001)

32. Cox T.J., D'Antonio P. "Acoustic absorbers and diffusers. Theory, design and application". 2 ed. Chapter 5. Taylor and Francis. (2009)

33. Carrión A. "Diseño acústico de espacios arquitectónicos". Chapter 2. Edicions UPC. (1998)

34. ISO 354: 2003. "Acoustics – Measurement of sound absorption in a reverberation room". (2003)

35. Jeong C-H. "Guideline for Adopting the Local Reaction Assumption for Porous Absorbers in Terms of Random Incidence Absorption Coefficients". Acta Acustica united with Acustica. Vol. 97, no 5. (2011)

36. Jeong C-H. “Converting Sabine absorption coefficients to random incidence absorption coefficients”. The Journal of the Acoustical Society of America. Vol. 133, no 6. (2013)

37. ISO 10354 – 2: 1998. “Acoustics – Determination of sound absorption coefficient and impedance in impedance tubes – Part 2: Transfer-function method”. (1998)

38. ISO 18233: 2006. “Acoustics – Application of new measurement methods in building and room acoustics”. (2006)

39. IEC 61260. “Electroacoustics – Octave-band and fractional-octave-band filters”. (1995)

40. Torras Rosell A. “Methods of measuring Impulse Responses in Architectural Acoustics”. DTU Master Thesis. (2009)

41. Rindel J.H. ”Modelling the Angle-Dependent Pressure Reflection Factor”. Applied Acoustics. Vol. 38, no 2-4. (1993)

42. Nilsson E. “Decay processes in rooms with non-diffuse sound fields. Part I: Ceiling Treatment with absorbing material”. Building Acoustics. Vol. 11, no 1. (2004)

43. Nilsson E. “Decay processes in rooms with non-diffuse sound fields. Part I: Effect of irregularities”. Building Acoustics. Vol. 11, no 2. (2004)

www.elektro.dtu.dk

Department of Electrical Engineering
Technical University of Denmark
Ørsteds Plads
Building 348
DK-2800 Kgs. Lyngby
Denmark
Tel: (+45) 45 25 38 00
Fax: (+45) 45 93 16 34
Email: info@elektro.dtu.dk